

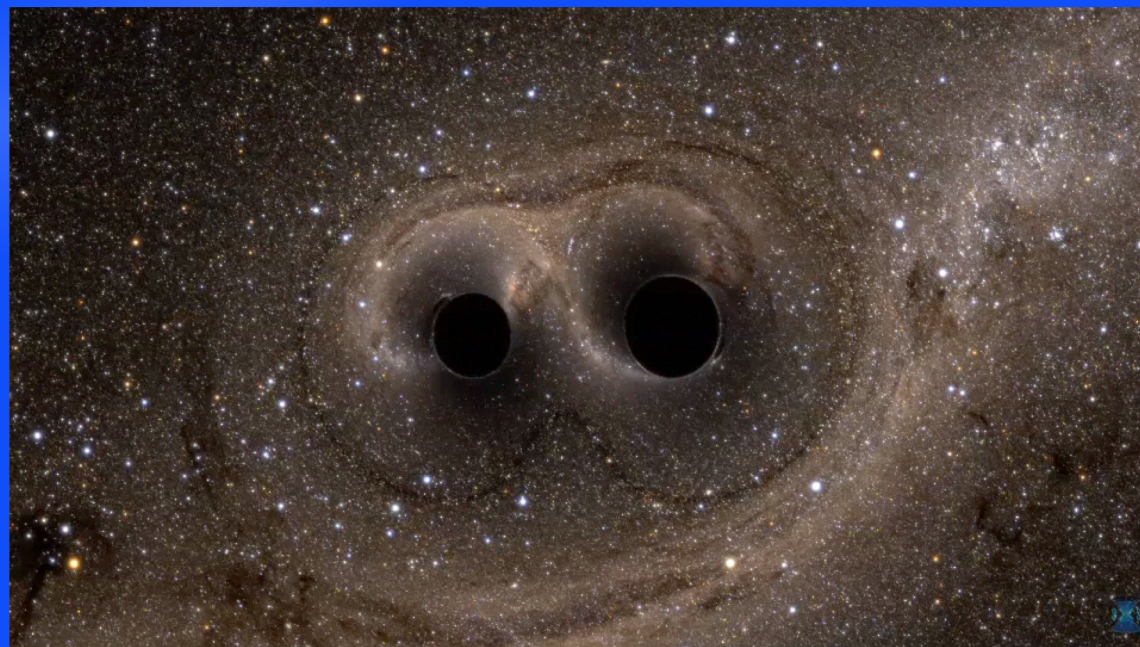


Gravitational Waves from Compact Binary Mergers seen by LIGO and Virgo

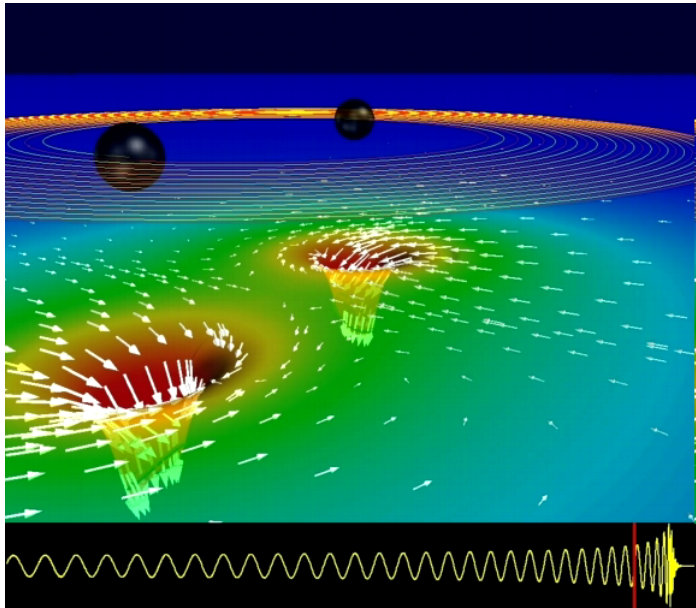
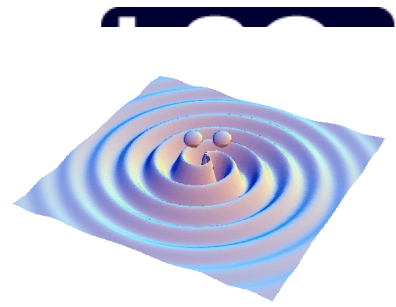
Alan J Weinstein
LIGO Laboratory, Caltech
for the LIGO and Virgo Collaborations
LIGO-Virgo Open Data Workshop
March 25, 2018



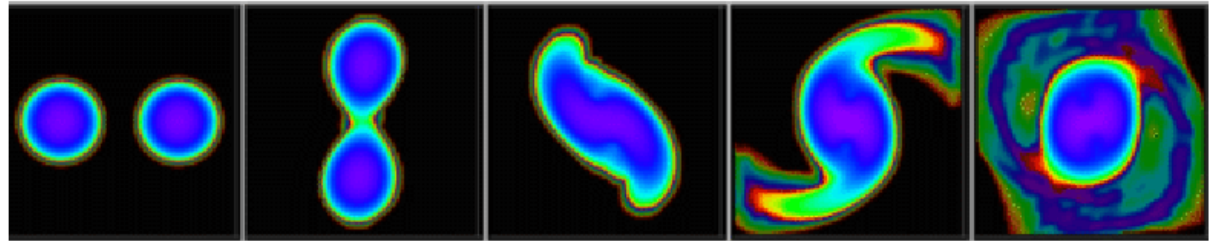
Caltech



LIGO GWs from coalescing compact binaries (NS/NS, BH/BH, NS/BH)

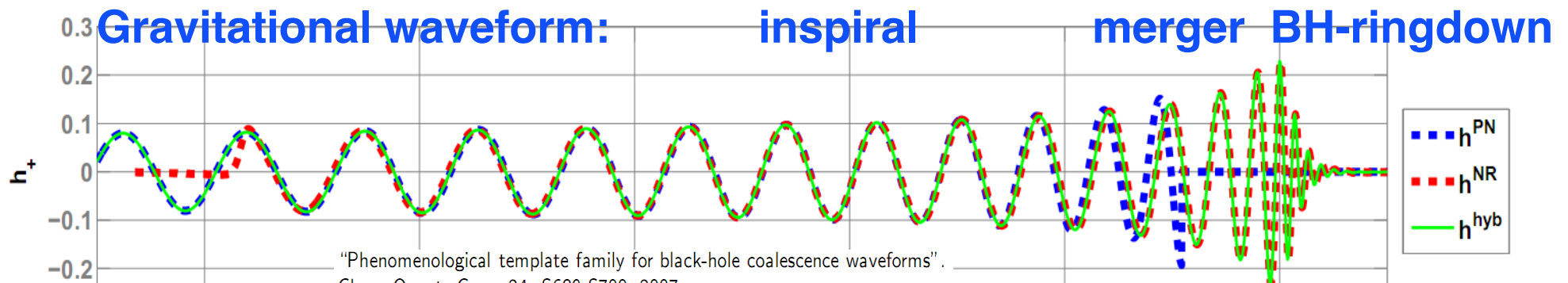


- Neutron star – neutron star (Centrella et al.)



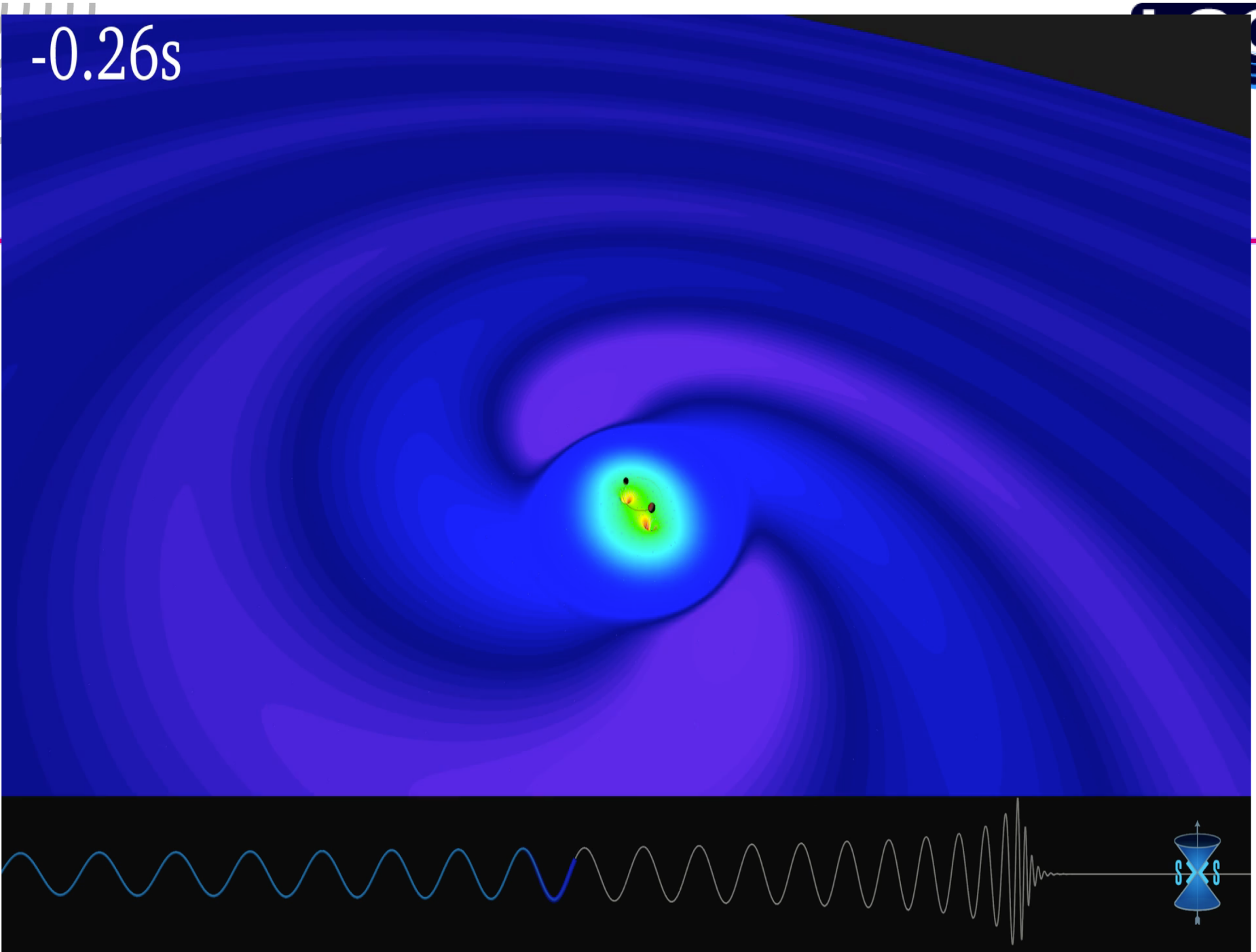
Tidal disruption of neutron star

A unique and powerful laboratory to study strong-field, highly dynamical gravity and the structure of nuclear matter in the most extreme conditions



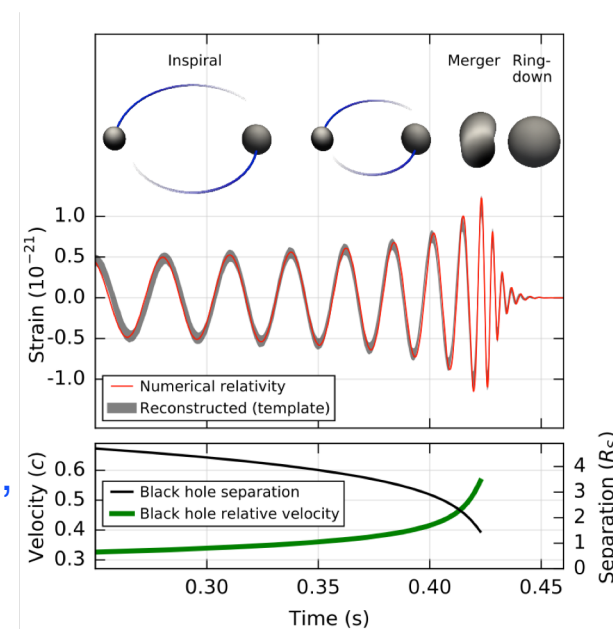
Waveform carries lots of information about binary masses, orbit, merger

-0.26s



CBC waveforms

- General Relativity can be used to solve the “two body problem” in dynamical gravity – a GW waveform that carries information about the orbit, inspiral, merger and ringdown of a binary black hole system. It took decades to solve this problem!
- Waveforms depend on a long list of “parameters” – see next slides.
- For systems involving neutron stars, “matter effects” are important in the last fraction of a second before merger (tidal distortion & disruption, formation of a merged hyper-massive neutron star, ...)
- If GR is not the correct theory of gravity in this highly strong-field, rapidly changing regime, this will be reflected in the observed waveform.
- Waveforms are used as:
 - » Templates for search template bank
 - » Parameter estimation via MCMC
 - » Estimating detector sensitivity (eg, BNS range)
 - » Testing search and PE pipelines with software and hardware injections
 - » Tools for modeling matter effects, beyond-GR effects, as governed by extra parameters

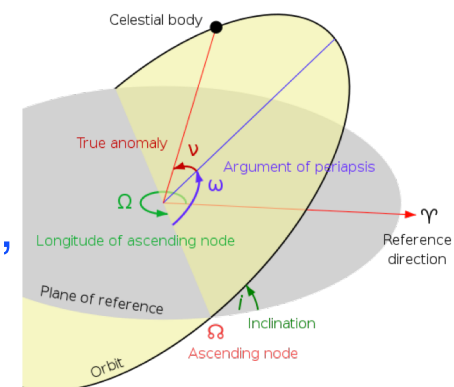


CBC waveforms in GR: parameters

- Two Component masses: m_1, m_2
- Six component spins: \vec{S}_1, \vec{S}_2
- 2-D sky location: right ascension α , declination δ
- Luminosity distance: d_L
- Orbital plane: inclination $\iota \cong \theta_{LN}$, polarization angle ψ
 - » If component spins are not aligned with the orbital angular momentum L , the orbital plane will *precess* about $\vec{J} = \vec{L} + \vec{S}_1 + \vec{S}_2$, so the inclination angle is θ_{JN} , and the precession dynamics must be computed properly!
- At coalescence: phase φ_c , time t_c
 - » Coalescence is defined by convention; eg, waveform peak of $h \sim |\cos\varphi + i \sin\varphi|$
- That's 15 parameters (so far), for (adiabatically) quasi-circular orbits

CBC waveforms in GR: more parameters

- Eccentricity: Gravitational radiation circularizes eccentric orbits, long before it gets into the LIGO band (> 10 orbits/s); but if the binary is formed (eg, through dynamical capture) in a tight eccentric orbit, already in the LIGO band, three more parameters are needed to describe eccentric orbits: eccentricity, angular location and orbital phase of periapsis.
- More parameters required to describe:
 - » tidal distortion and disruption of neutron stars,
 - » Hyper-massive massive neutron star (HMNS) properties,
 - » beyond-GR effects; *e.g.*,
 - deviations of post-Newtonian expansion as $v/c \rightarrow 1$
 - Disagreement between observed final BH mass and spin from predictions from component masses and spins
 - Deviations of final BH higher-order mode spectrum (frequencies, damping times) from BHPT prediction



CBC waveforms

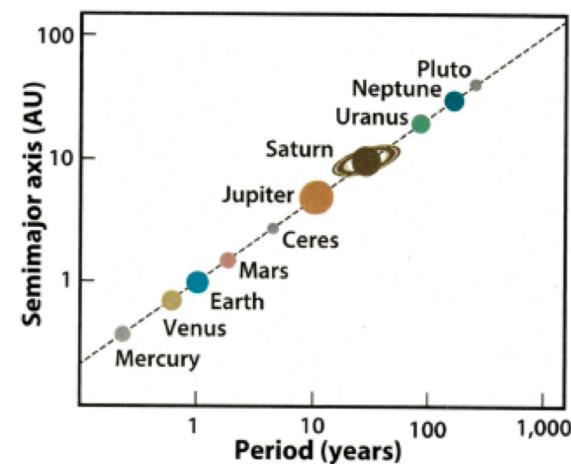
- Three phases: Inspiral, merger, ringdown
- The (early) inspiral phase can be computed as a “post-Newtonian” expansion in powers of (v/c) , where v is the orbital velocity of the binary, by taking into account the orbital energy and the flux (energy and angular momentum loss) of emitted GWs that cause the orbit to shrink towards merger

- Kepler’s 3rd law: $\omega_{orb}^2 r_{orb}^3 = GM_{tot}$

- $\omega_{orb} = 2\pi f_{orb} = \pi f_{GW}$,

$$v_{orb} = \omega_{orb} r_{orb} \Rightarrow$$

$$v_{orb}^3 = \pi GM_{tot} f_{GW}$$



ASTRONOMY: RICHARD TALCOTT AND ROEN KELLY

Binary inspiral in the PN expansion

- PN orbital energy:

$$E = -\frac{\nu M v^2}{2} \left\{ 1 + \left(-\frac{9 + \nu}{12} \right) v^2 + \left(\frac{-81 + 57\nu - \nu^2}{24} \right) v^4 + \left(-\frac{675}{64} + \left[\frac{34445}{576} - \frac{205\pi^2}{96} \right] \nu - \frac{155}{96} \nu^2 - \frac{35}{5184} \nu^3 \right) v^6 + \mathcal{O}(v^8) \right\},$$

and

$$\mathcal{F} = \frac{32\nu^2 v^{10}}{5} \left\{ 1 - \left(\frac{1247}{336} + \frac{35}{12} \nu \right) v^2 + 4\pi v^3 + \left(-\frac{44711}{9072} + \frac{9271}{504} \nu + \frac{65}{18} \nu^2 \right) v^5 \dots \right.$$

- PN energy loss:

- GW strain, time domain:

$$h_+ = \frac{2\nu M}{D} v^2 (1 + \cos^2 \iota) \cos[2\varphi(t)], \quad h_\times = \frac{4\nu M}{D} v^2 \cos \iota \sin[2\varphi(t)],$$

$$\frac{d\varphi(t)}{dt} = \frac{v^3}{M}, \quad \frac{dv}{dt} = \frac{-\mathcal{F}(v)}{E'(v)}.$$

- PN waveform phase

$$v = \pi M f_{\text{gw}} \quad \text{and} \quad \tau = [\nu(t_C - t)/(5M)]^{-1/8}$$

$$\begin{aligned} \varphi(t) = & \frac{-1}{\nu\tau^5} \left\{ 1 + \left(\frac{3715}{8064} + \frac{55}{96} \nu \right) \tau^2 - \frac{3\pi}{4} \tau^3 + \left(\frac{9275495}{14450688} + \frac{284875}{258048} \nu + \frac{1855}{2048} \nu^2 \right) \tau^4 \right. \\ & + \left(-\frac{38645}{172032} + \frac{65}{2048} \nu \right) \pi \tau^5 \ln \tau + \left[\frac{831032450749357}{57682522275840} - \frac{53}{40} \pi^2 - \frac{107}{56} (\gamma + \ln(2\tau)) \right. \\ & + \left(-\frac{126510089885}{4161798144} + \frac{2255}{2048} \pi^2 \right) \nu + \frac{154565}{1835008} \nu^2 - \frac{1179625}{1769472} \nu^3 \left. \right] \tau^6 \\ & \left. + \left(\frac{188516689}{173408256} + \frac{488825}{516096} \nu - \frac{141769}{516096} \nu^2 \right) \pi \tau^7 \right\}, \end{aligned}$$

- Or you can easily do it numerically!

Sathyaprakash & Schutz

Living Rev. Relativity, **12**, (2009), 2

<http://www.livingreviews.org/lrr-2009-2>

GW strain in the frequency domain:

$$\tilde{h}(f) = H(f) = \mathcal{A} f^{-7/6} \exp \left[i \Psi(f) + i \frac{\pi}{4} \right], \quad (127)$$

with the Fourier amplitude \mathcal{A} and phase $\Psi(f)$ given by

$$\mathcal{A} = \frac{\mathcal{C}}{D \pi^{2/3}} \sqrt{\frac{5\nu}{24}} M^{5/6}, \quad \Psi(f) = 2\pi f t_C + \Phi_C + \frac{3}{128\nu} \sum_k \alpha_k (\pi M f)^{(k-5)/3}. \quad (128)$$

Here ν is the symmetric mass ratio defined before (see Equation 31), \mathcal{C} is a function of the various angles, as in Equation (124), and t_C and Φ_C are the fiducial epoch of merger and the phase of the signal at that epoch, respectively. The coefficients in the PN expansion of the Fourier phase are given by

$$\begin{aligned} \alpha_0 &= 1, & \alpha_1 &= 0, & \alpha_2 &= \frac{3715}{756} + \frac{55}{9}\nu, & \alpha_3 &= -16\pi, \\ \alpha_4 &= \frac{15293365}{508032} + \frac{27145}{504}\nu + \frac{3085}{72}\nu^2, & \alpha_5 &= \pi \left(\frac{38645}{756} - \frac{65}{9}\nu \right) \left[1 + \ln \left(6^{3/2} \pi M f \right) \right], \\ \alpha_6 &= \frac{11583231236531}{4694215680} - \frac{640}{3}\pi^2 - \frac{6848}{21}\gamma + \left(-\frac{15737765635}{3048192} + \frac{2255}{12}\pi^2 \right) \nu \\ &\quad + \frac{76055}{1728}\nu^2 - \frac{127825}{1296}\nu^3 - \frac{6848}{63} \ln(64\pi M f), \\ \alpha_7 &= \pi \left(\frac{77096675}{254016} + \frac{378515}{1512}\nu - \frac{74045}{756}\nu^2 \right). \end{aligned} \quad (129)$$

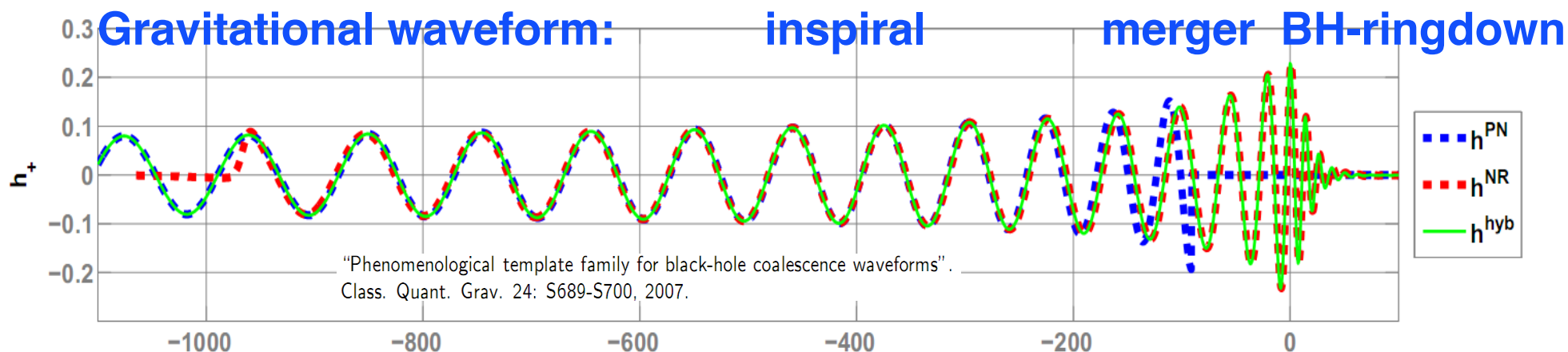
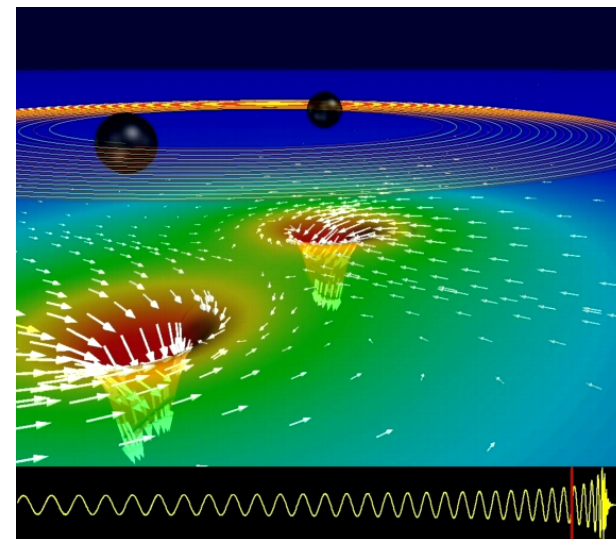
Sathyaprakash & Schutz

Living Rev. Relativity, **12**, (2009), 2

<http://www.livingreviews.org/lrr-2009-2>

Merger and ringdown

- The PN expansion fails as $(v/c) \rightarrow 1$, BBH merger
- After merger, the final merged black hole rings down, as described by BH perturbation theory.
- In between (inspiral \rightarrow merger \rightarrow ringdown), full GR is required. No analytical solution is known!
- Instead, numerically solve the GR field equations through (extremely compute-intensive) simulations (numerical relativity, NR).
- These simulations take months, even for just a few orbits.
- To produce waveforms that span many orbits, “stitch” PN inspiral to NR-simulated merger-ringdown waveforms – “hybridization”.



Black hole ringdown

- The final, merged BH is highly perturbed; it radiates its excess energy in a GW “ringdown”, in a series of “quasi-normal modes” (QNMs) – BH *spectroscopy*.
- The higher order modes have not yet been observed!

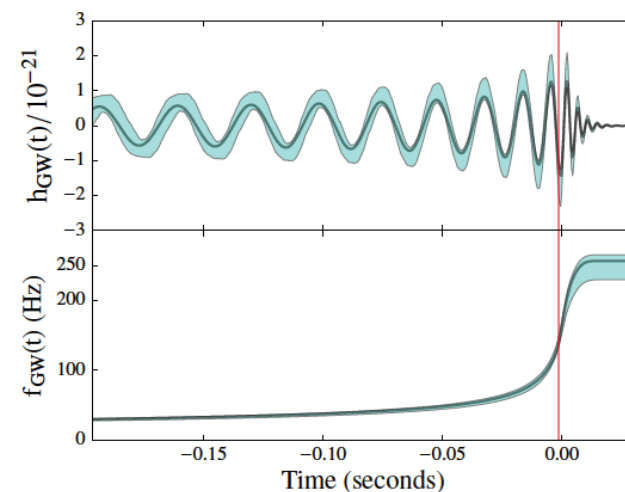
$$h_+ = \frac{A(f_{lmn}, Q_{lmn}, \epsilon_{rd})}{r} (1 + \cos^2 \iota) \exp\left(\frac{-\pi f_{lmn} t}{Q_{lmn}}\right) \cos(2\pi f_{lmn} t + \varphi_{lmn}),$$

$$h_\times = \frac{A(f_{lmn}, Q_{lmn}, \epsilon_{rd})}{r} 2 \cos \iota \exp\left(\frac{-\pi f_{lmn} t}{Q_{lmn}}\right) \sin(2\pi f_{lmn} t + \varphi_{lmn}),$$

$$Q_{lmn} = \omega_{lmn} \tau_{lmn} / 2 :$$

$$l = 2, m = n = 0$$

$$f_{200} = \pm 1.207 \times 10^3 \frac{10 M_\odot}{M} \text{ Hz}, \quad \tau_{200} = 5.537 \times 10^{-4} \frac{M}{10 M_\odot} \text{ s.}$$



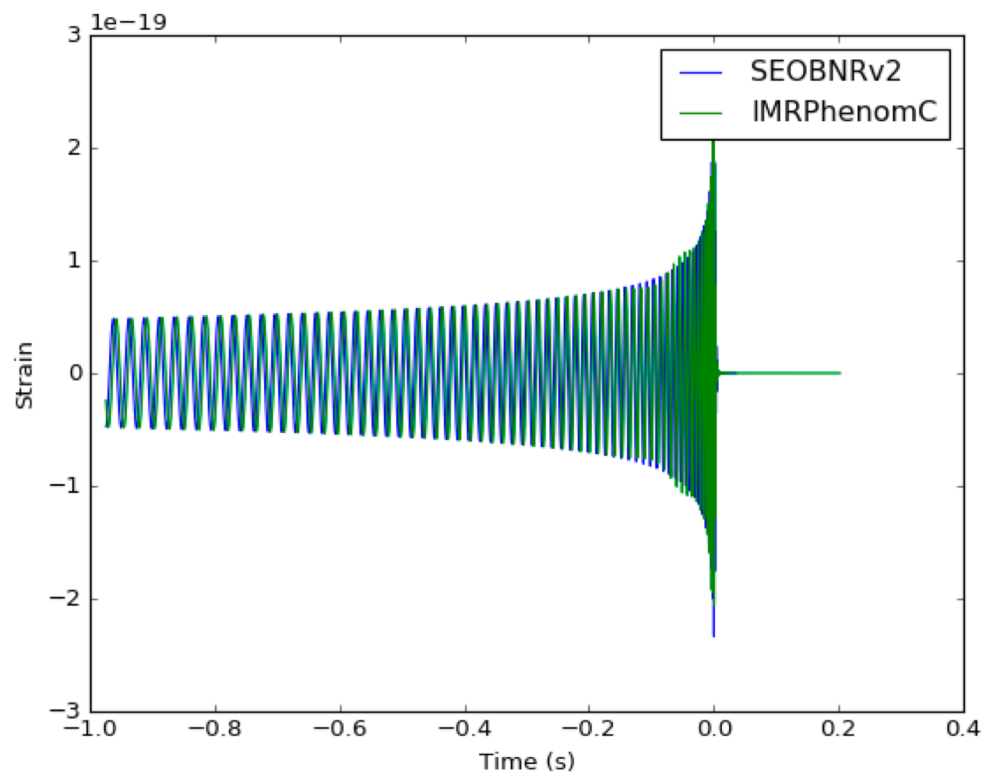
Parametrized waveform families

- For, eg, CBC parameter estimation, a Markov Chain Monte Carlo (MCMC) steps through this parameter space, repeatedly generating waveforms that are match-filtered against the data; waveform generation is a limiting step, and NR computations are prohibitively slow.
- Different groups have developed IMR waveform “families” which can be “quickly” computed from input parameters (10 parameters for quasi-circular orbits with aligned component spins; up to 15 parameters for generic spins – precessing orbits).
- Many waveform families have been developed (PN, NR, eccentric orbits, tides, NEOS, etc).
- For the BBH search and parameter estimation pipelines, popular waveform families include:
 - » IMRPhenomB – “phenomenological” model, aligned spins
 - » IMRPhenomP – “phenomenological” model, non-aligned spins (precession)
 - » SEOBNRv4 – Based on the “equivalent one-body” formalism, with parameterized M-R from NR “stitched on”; aligned spins

- ```
$ python ../examples/waveform/what_waveform.py
 ['TEOBResum_ROM', 'TaylorEt', 'SEOBNRv3_opt', 'IMRPhenomA', 'IMRPhenomC', 'IMRPhenomB', 'EOBNRv2', 'NRSur7dq2', 'TEOBv4',
 'SEOBNRv4_opt', 'PhenSpinTaylor', 'PhenSpinTaylorRD', 'NR_hdf5', 'TEOBv2', 'SEOBNRv3_pert', 'EOBNRv2HM', 'SpinTaylorT4', 'TaylorT1',
 'TaylorT3', 'TaylorT2', 'HGimri', 'TaylorT4', 'IMRPhenomD', 'IMRPhenomPv2', 'SEOBNRv1', 'SpinDominatedWf', 'SEOBNRv3', 'SEOBNRv2',
 'SpinTaylorT1', 'SEOBNRv4', 'SpinTaylorT2', 'EccentricTD', 'SEOBNRv2_opt', 'SEOBNRv3_opt_rk4'] ['IMRPhenomD_NRTidal', 'TaylorF2',
 'SEOBNRv2_ROM_EffectiveSpin', 'IMRPhenomA', 'IMRPhenomC', 'IMRPhenomB', 'IMRPhenomD', 'SpinTaylorT2Fourier', 'IMRPhenomPv2_INTERP',
 'SpinTaylorT4Fourier', 'TaylorF2NLTides', 'IMRPhenomD_INTERP', 'SEOBNRv2_ROM_DoubleSpin', 'IMRPhenomP', 'SEOBNRv4_ROM_NRTidal',
 'SpinTaylorF2', 'SEOBNRv2_ROM_DoubleSpin_INTERP', 'SEOBNRv1_ROM_DoubleSpin_INTERP', 'EOBNRv2_ROM_INTERP', 'TaylorF2_INTERP',
 'SEOBNRv2_ROM_DoubleSpin_HI', 'SpinTaylorF2_INTERP', 'TaylorF2NL_INTERP', 'EOBNRv2_ROM', 'SEOBNRv1_ROM_EffectiveSpin',
 'SEOBNRv1_ROM_DoubleSpin', 'TaylorF2NL', 'EccentricFD', 'SpinTaylorF2_SWAPPER_INTERP', 'SEOBNRv4_ROM',
 'SEOBNRv1_ROM_EffectiveSpin_INTERP', 'EOBNRv2HM_ROM', 'EOBNRv2HM_ROM_INTERP', 'TaylorF2RedSpinTidal', 'IMRPhenomPv2',
 'SEOBNRv4_ROM_INTERP', 'TaylorF2RedSpin', 'Lackey_Tidal_2013_SEOBNRv2_ROM', 'IMRPhenomC_INTERP', 'SEOBNRv2_ROM_EffectiveSpin_INTERP',
 'NRSur4d2s', 'SEOBNRv2_ROM_DoubleSpin_HI_INTERP', 'SpinTaylorF2_SWAPPER']
```

# Subtle (but important!) differences between waveform families

- If we knew which waveform family(s) were “right” (most accurate representation of GR prediction), we’d just use them...
- But we don’t.
- Different waveform families can help us estimate the “systematic error” associated with our imperfect knowledge of the correct GR prediction.
- This is crucial for testing GR!



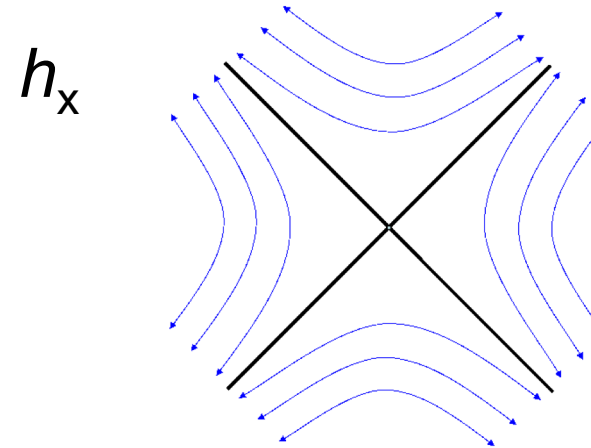
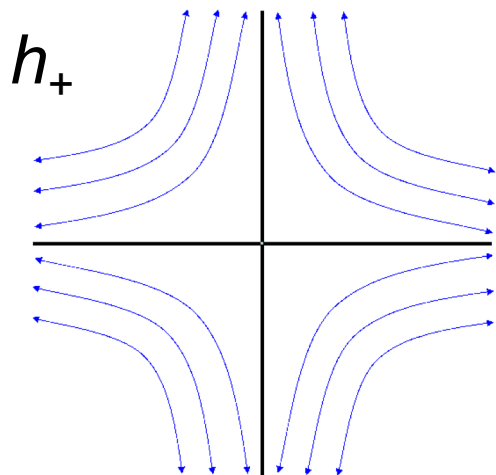
# Gravitational Wave Polarization

Solution for an outward propagating wave in z-direction:

$$h(t, z) = h_{\mu\nu} e^{i(\omega t - kz)} = h_+(t - z/c) + h_x(t - z/c)$$

$$h_{\mu\nu} = \begin{pmatrix} 0 & 0 & 0 & 0 \\ 0 & h_+ & h_x & 0 \\ 0 & h_x & -h_+ & 0 \\ 0 & 0 & 0 & 0 \end{pmatrix}$$

$$h_{\mu\nu} \approx \frac{1}{r} \frac{G}{c^4} \ddot{I}_{\mu\nu}$$



## Frames of reference:

- Detector coordinate frame
- Radiation coordinate frame
- Celestial coordinates (source coordinates)
- Geographic coordinates (detectors on the Earth)

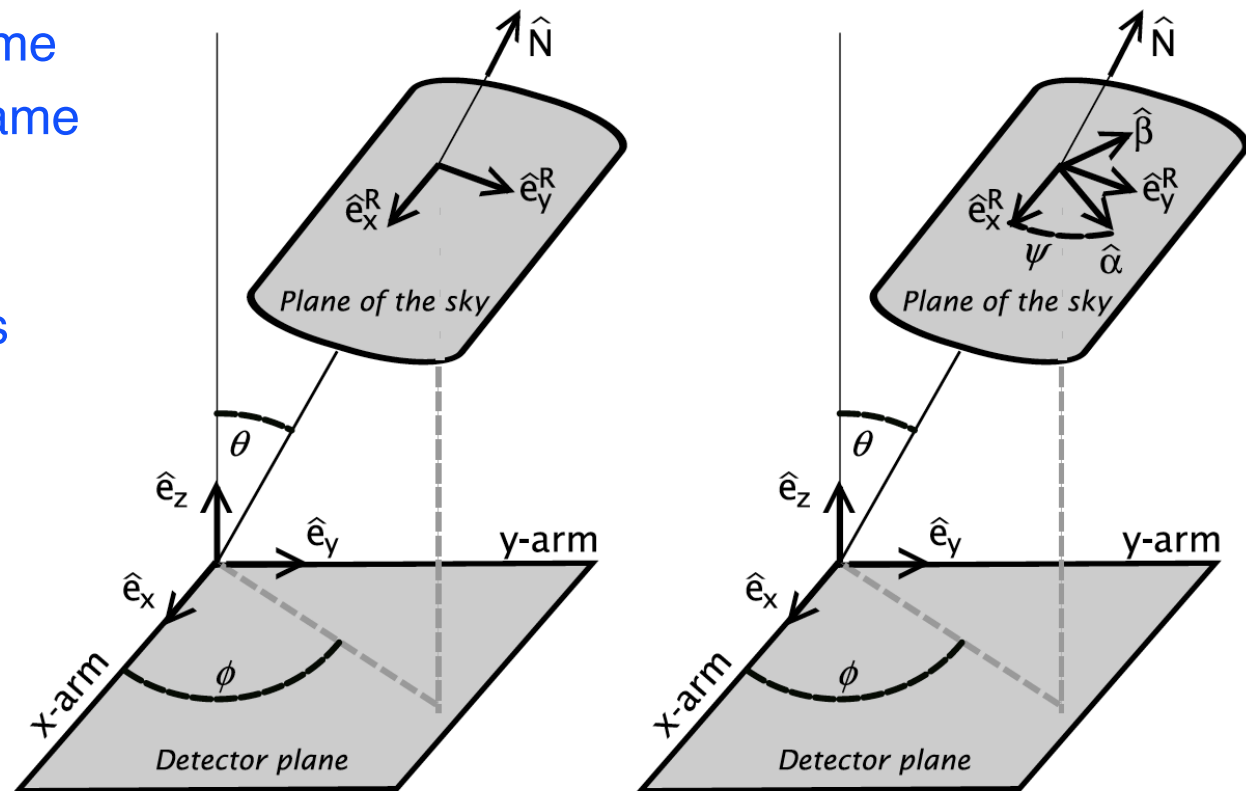


**Figure 3:** The relative orientation of the sky and detector frames (left panel) and the effect of a rotation by the angle  $\psi$  in the sky frame (left panel).

Sathyaprakash & Schutz

*Living Rev. Relativity*, **12**, (2009), 2

<http://www.livingreviews.org/lrr-2009-2>

# Computing the detector response

- Strain tensor, two polarizations:

$$\mathbf{h}(t) = h_+(t)\mathbf{e}_+ + h_\times(t)\mathbf{e}_\times,$$

$$h_{\mu\nu} = \begin{pmatrix} 0 & 0 & 0 & 0 \\ 0 & h_+ & h_\times & 0 \\ 0 & h_\times & -h_+ & 0 \\ 0 & 0 & 0 & 0 \end{pmatrix}$$

$$\mathbf{e}_+ = (\hat{e}_x^R \otimes \hat{e}_x^R - \hat{e}_y^R \otimes \hat{e}_y^R), \quad \mathbf{e}_\times = (\hat{e}_x^R \otimes \hat{e}_y^R + \hat{e}_y^R \otimes \hat{e}_x^R).$$

- Detector response:

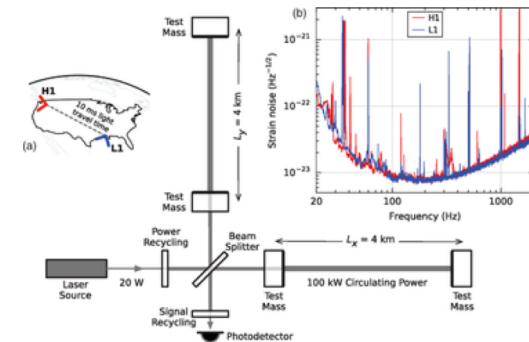
$$\left(\frac{d\delta t_{\text{return}}}{dt}\right) = \left(\frac{dt_{\text{return}}}{dt}\right)_{\text{x-arm}} - \left(\frac{dt_{\text{return}}}{dt}\right)_{\text{y-arm}} = L\hat{e}_x \cdot \dot{\mathbf{h}} \cdot \hat{e}_x - L\hat{e}_y \cdot \dot{\mathbf{h}} \cdot \hat{e}_y$$

- Detector tensor:

$$\mathbf{d} = L(\hat{e}_x \otimes \hat{e}_x - \hat{e}_y \otimes \hat{e}_y).$$

- Detector response as a tensor “inner product”:

$$\delta t_{\text{return}}(t) = \mathbf{d} : \mathbf{h}.$$





# Antenna response functions

- Detector response in terms of antenna pattern:

$$h_{\text{det}}(t) = \frac{\delta L(t)}{L} = F_+(\theta, \phi, \psi)h_+(t) + F_\times(\theta, \phi, \psi)h_\times(t),$$

- Detector antenna response functions:

$$F_+ \equiv \mathbf{d} : \mathbf{e}_+, \quad F_\times \equiv \mathbf{d} : \mathbf{e}_\times.$$

- In detector frame:

$$F_+ = \frac{1}{2} (1 + \cos^2 \theta) \cos 2\phi \cos 2\psi - \cos \theta \sin 2\phi \sin 2\psi,$$

$$F_\times = \frac{1}{2} (1 + \cos^2 \theta) \cos 2\phi \sin 2\psi + \cos \theta \sin 2\phi \cos 2\psi.$$

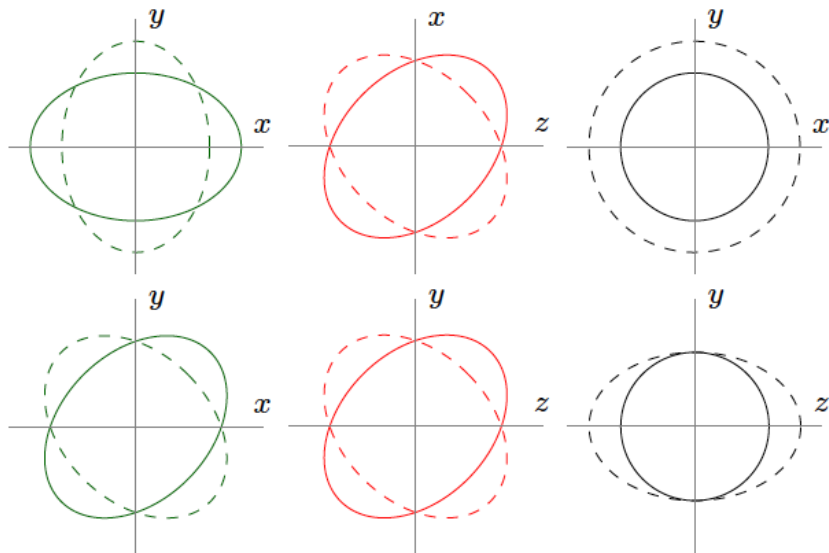
- These formulae are rarely used. Easier to work with radiation tensor and detector tensor, in celestial coordinates

# Non-tensor polarization

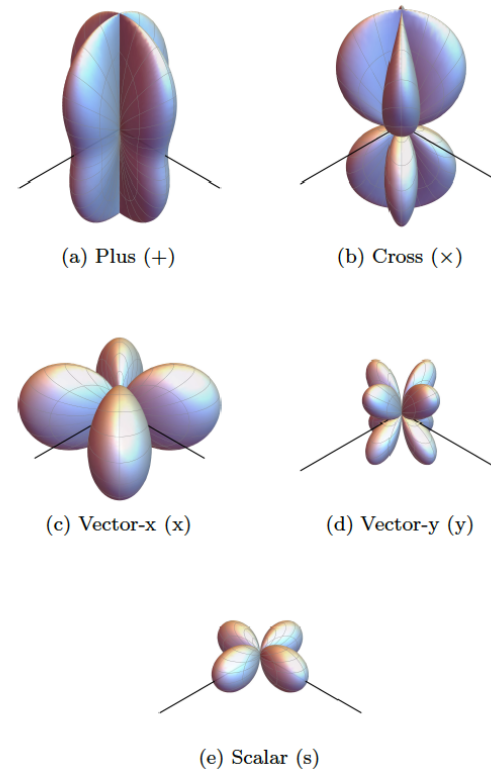
(Spatial part of the)  
general metric field  
tensor:

$$[h_{ij}] = \begin{pmatrix} h_b + h_+ & h_x & h_x \\ h_x & h_b - h_+ & h_y \\ h_x & h_y & h_l \end{pmatrix}$$

Effect on a ring of test masses:



Antenna patterns:

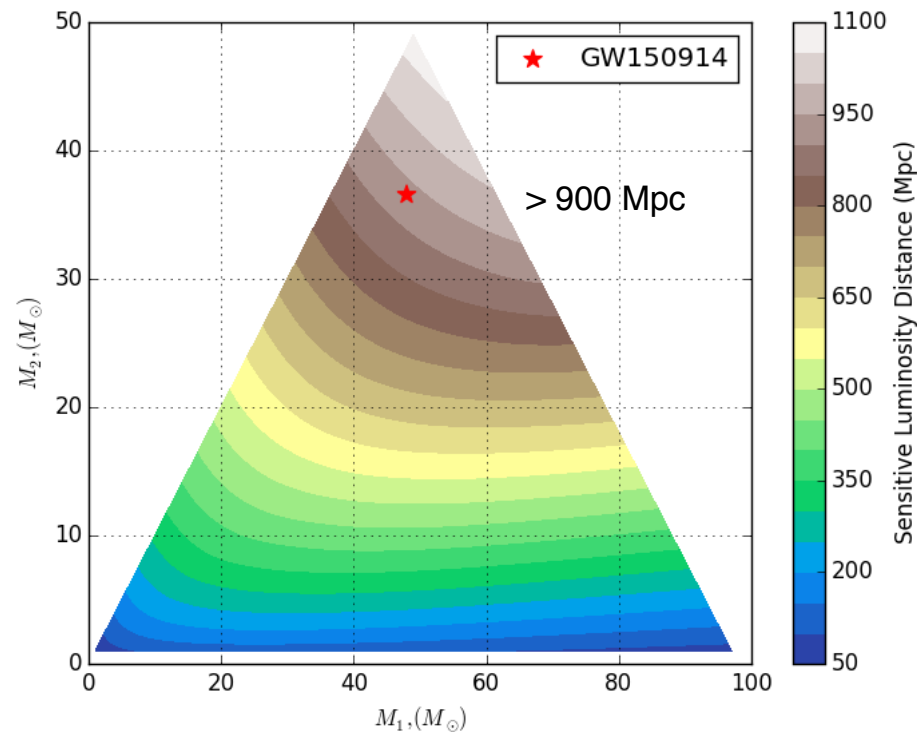
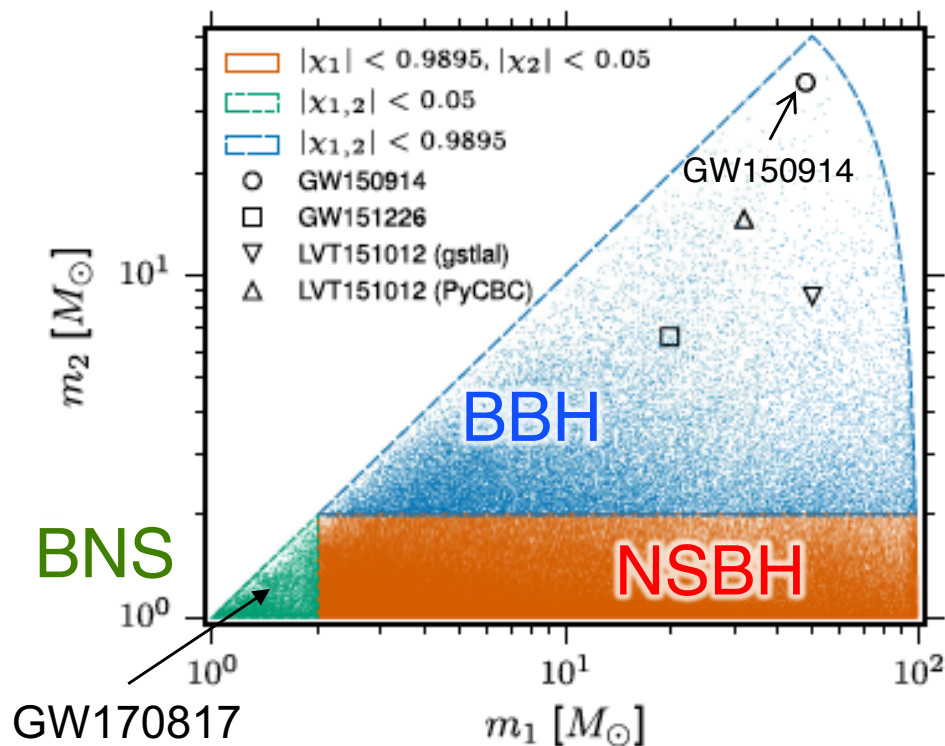


# Search pipelines

---

- We need to sift through months of two-detector-coincident strain data  $h(t)$  to look for signals with durations from minutes to fractions of a second, above the detector noise.
- **Two different template-based searches for compact binary coalescence (CBC): BNS, NSBH, BBH:**
  - » Low-latency (10's of seconds) – gstlal (gstreamer-based)
  - » “Offline” and “Live” - pyCBC (fft-based)
- **Two different searches for short-duration, unmodeled “bursts” of GW power in the time-frequency plane, with low latency:**
  - » Coherent WaveBurst - cWB
  - » Online LIGO Inference Burst – oLIB
- All make use of **two-detector coincidence in time and in signal morphology**.
- All estimate the background from accidental coincidence of instrumental noise triggers, using “time slides” or variations thereof.
- **All detected GW150914 and the other LIGO-Virgo detected events, with high significance above detector noise**

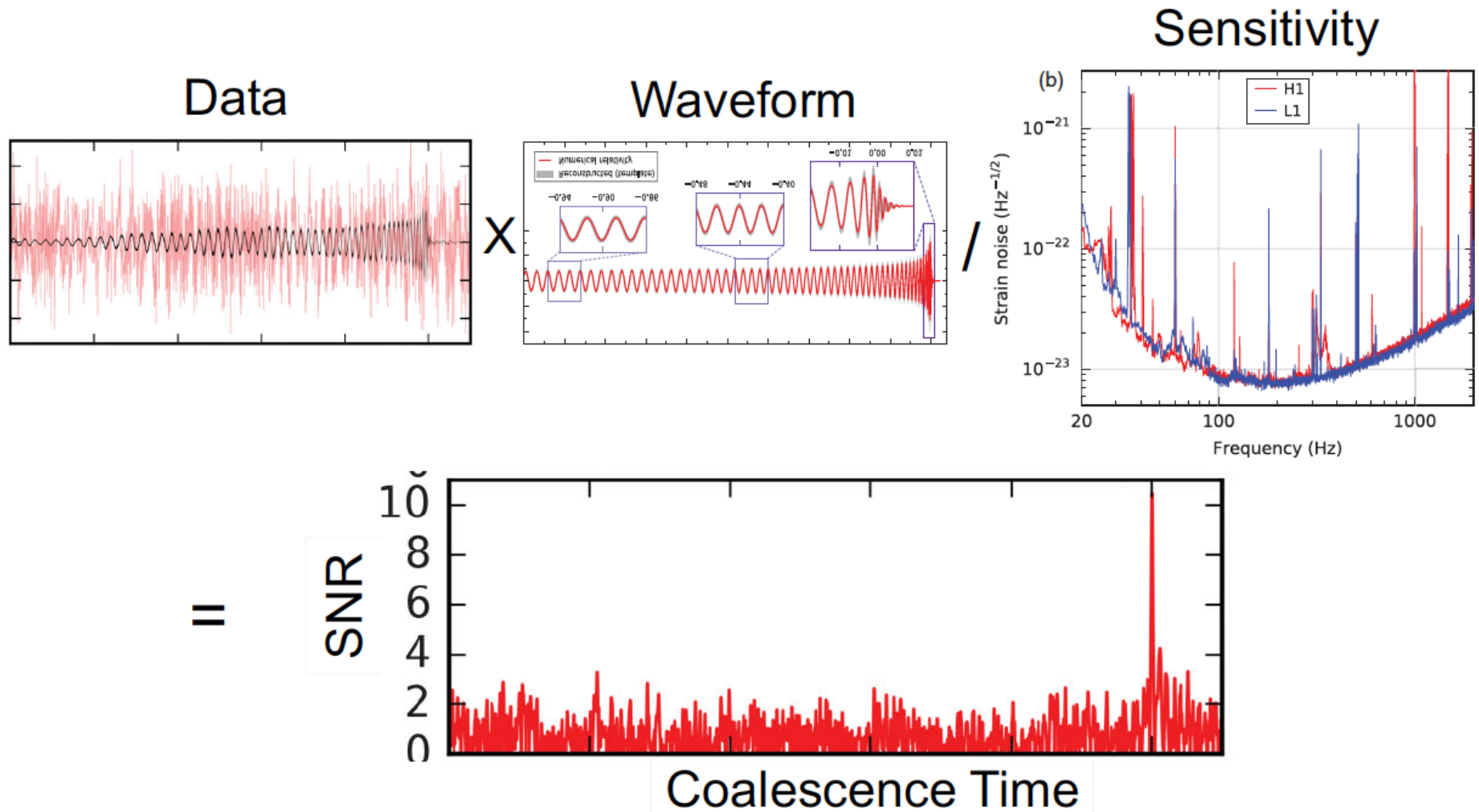
# Template-based searches



Masses and (aligned) spins  
 Templates spaced for  $< 3\%$   
 loss of SNR: 250K templates.

Sensitive distance in Mpc

# Matched Filtering in the time domain



# Matched filtering in the frequency domain

For each template  $h(t)$  and for the strain data from a single detector  $s(t)$ , the analysis calculates the square of the matched-filter SNR defined by [12]

$$\rho^2(t) \equiv \frac{1}{\langle h|h \rangle} | \langle s|h \rangle(t) |^2, \quad (1)$$

where the correlation is defined by

$$\langle s|h \rangle(t) = 4 \int_0^\infty \frac{\tilde{s}(f)\tilde{h}^*(f)}{S_n(f)} e^{2\pi ift} df, \quad (2)$$

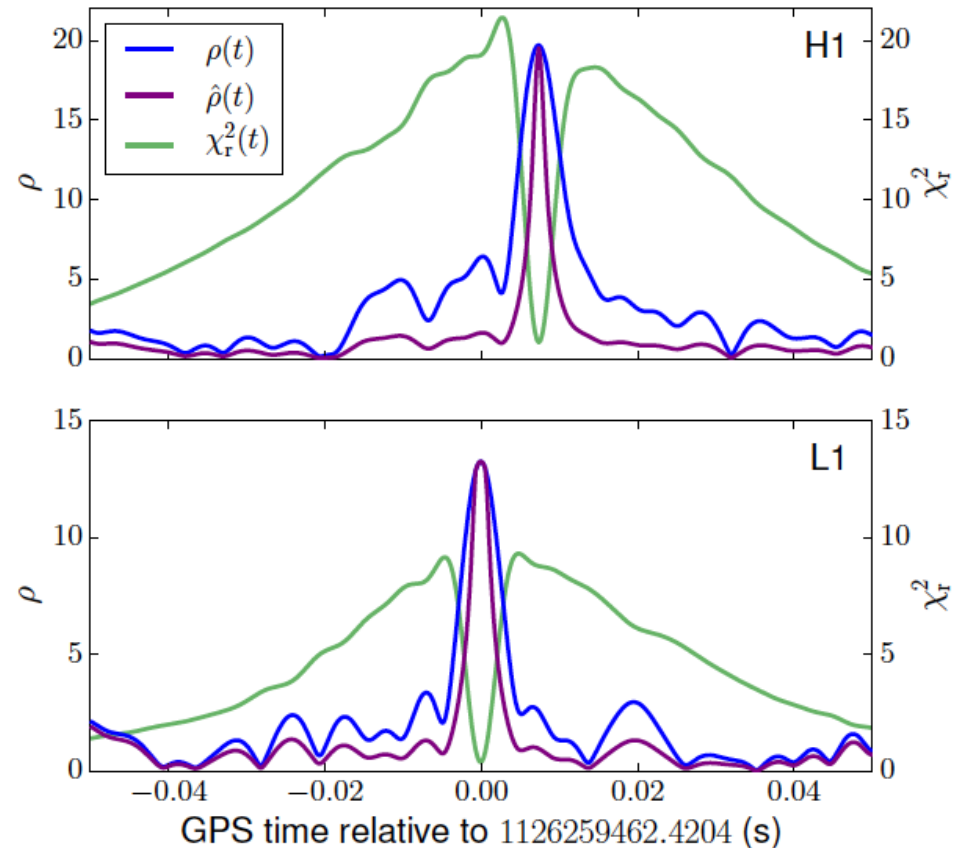
where  $\tilde{s}(f)$  is the Fourier transform of the time domain quantity  $s(t)$  given by

$$\tilde{s}(f) = \int_{-\infty}^\infty s(t)e^{-2\pi ift} dt. \quad (3)$$

The quantity  $S_n(|f|)$  is the one-sided average power spectral density of the detector noise, which is re-calculated every 2048 s (in contrast to the fixed spectrum used in template bank construction). Calculation of the matched-filter SNR in the frequency domain allows the use of the computationally efficient Fast Fourier Transform [85, 86]. The square of the matched-filter SNR in Eq. (1) is normalized by

$$\langle h|h \rangle = 4 \int_0^\infty \frac{\tilde{h}(f)\tilde{h}^*(f)}{S_n(f)} df, \quad (4)$$

so that its mean value is 2, if  $s(t)$  contains only stationary noise [87].



LVC, B. Abbott et al.,  
Phys. Rev. Lett. 116, 061102 –11 February 2016

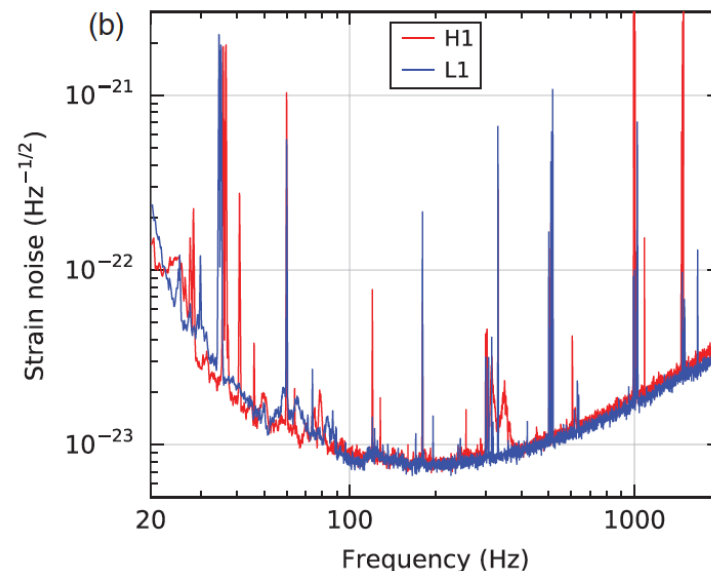
# Whitening in frequency domain

- The LIGO and Virgo detectors have lots of noise at low (< 20 Hz) and high (> 2000 Hz) frequencies.
- We will only be able to detect weak GWs in the “detection band” between 20 – 2000 Hz.
- The S/N ratio thus is most easily calculated in the frequency domain, weighting (dividing by) the noise power.

- SNR integrand =  $\frac{\tilde{s}(f)\tilde{h}^*(f)}{S(f)} = \left(\frac{\tilde{s}(f)}{\sqrt{S(f)}}\right) \left(\frac{\tilde{h}^*(f)}{\sqrt{S(f)}}\right)$

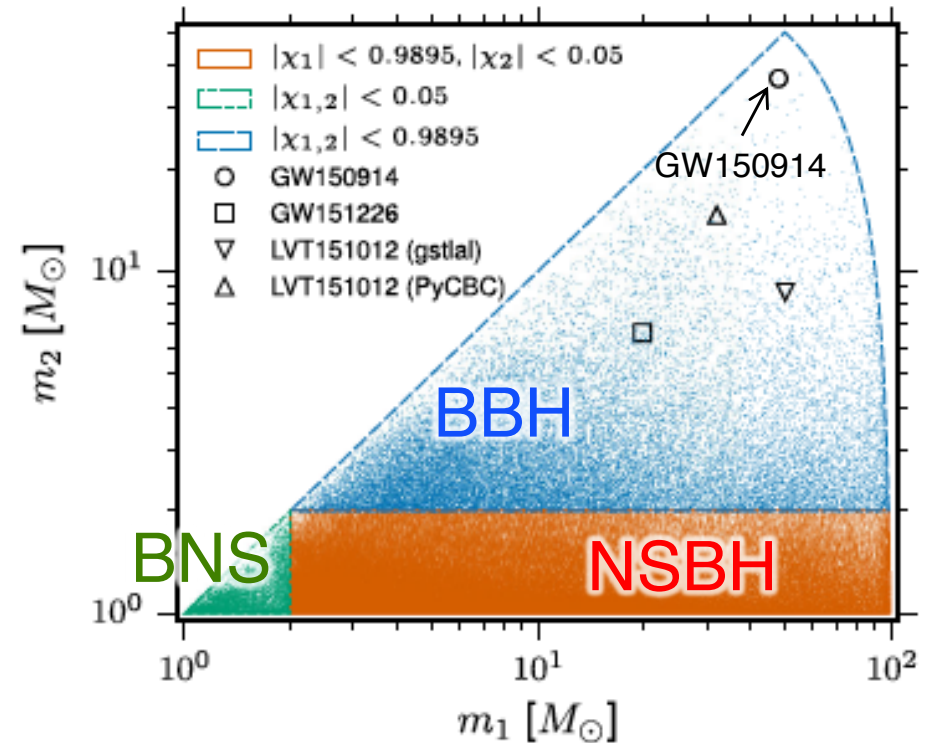
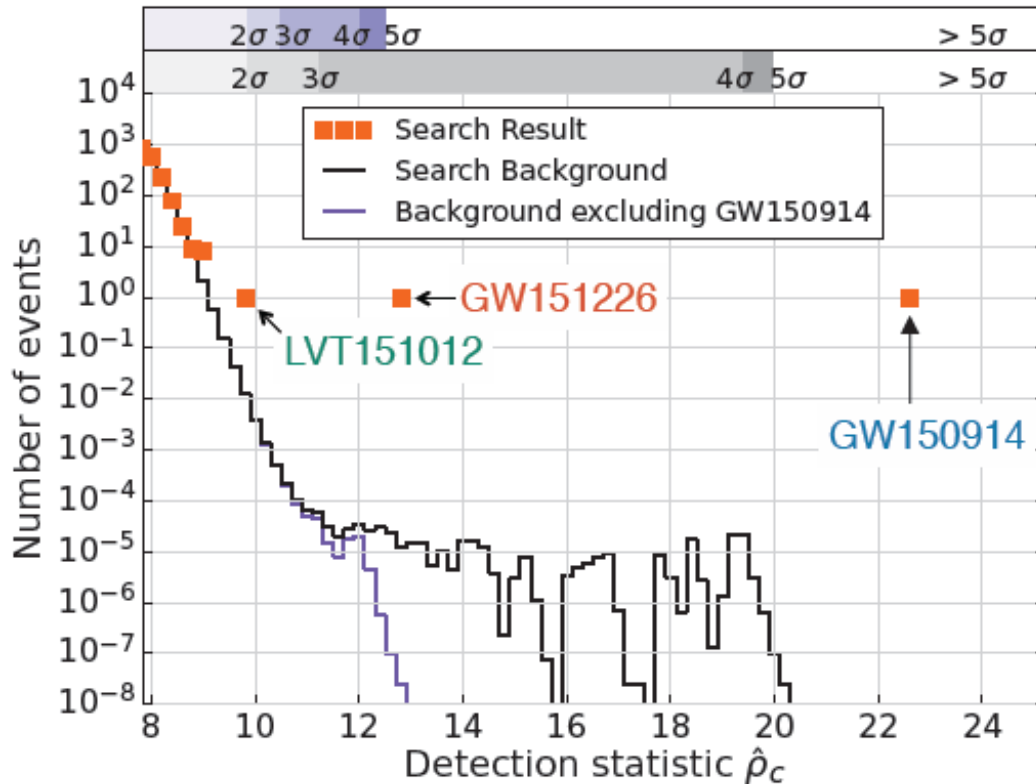
which is the *whitened* data times the *whitened* template.

- Whitening both of these is thus the first step in most any LIGO analysis.



$$\langle s|h \rangle(t) = 4 \int_0^\infty \frac{\tilde{s}(f)\tilde{h}^*(f)}{S_n(f)} e^{2\pi ift} df,$$

## Advanced LIGO Observing Run O1

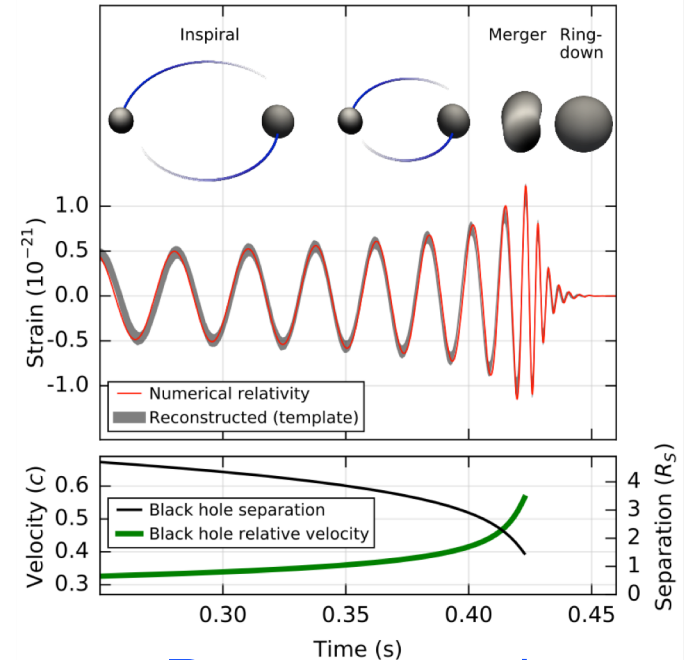
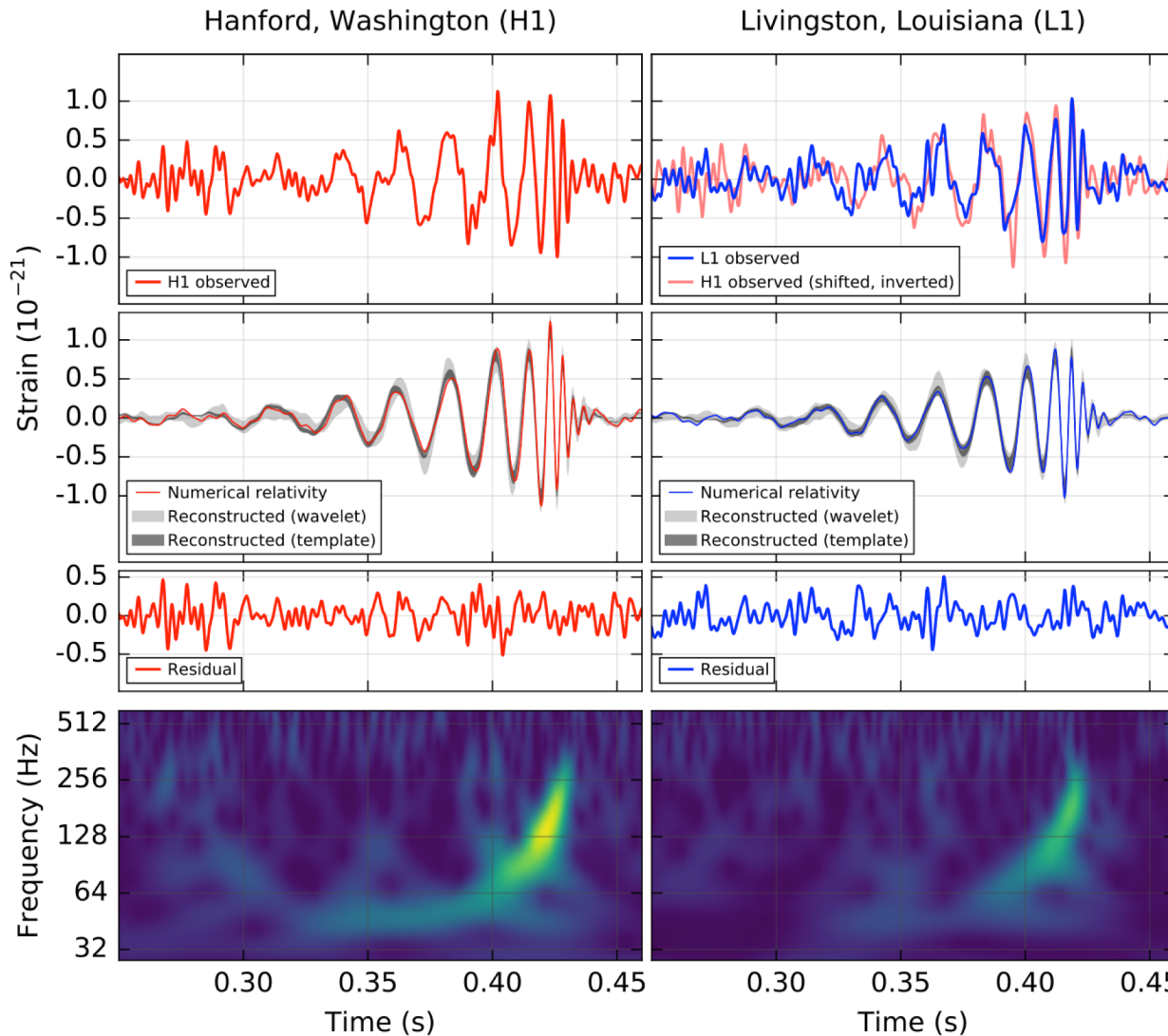


Three events above the estimated “background” from accidental coincidence of noise fluctuation triggers. Two have high significance ( $> 5\sigma$ ).



# GW150914

Phys. Rev. Lett. 116, 061102 – Published 11 February 2016  
<https://dcc.ligo.org/LIGO-P150914/public/main>



Reconstructed  
(no whitening)

Audio:

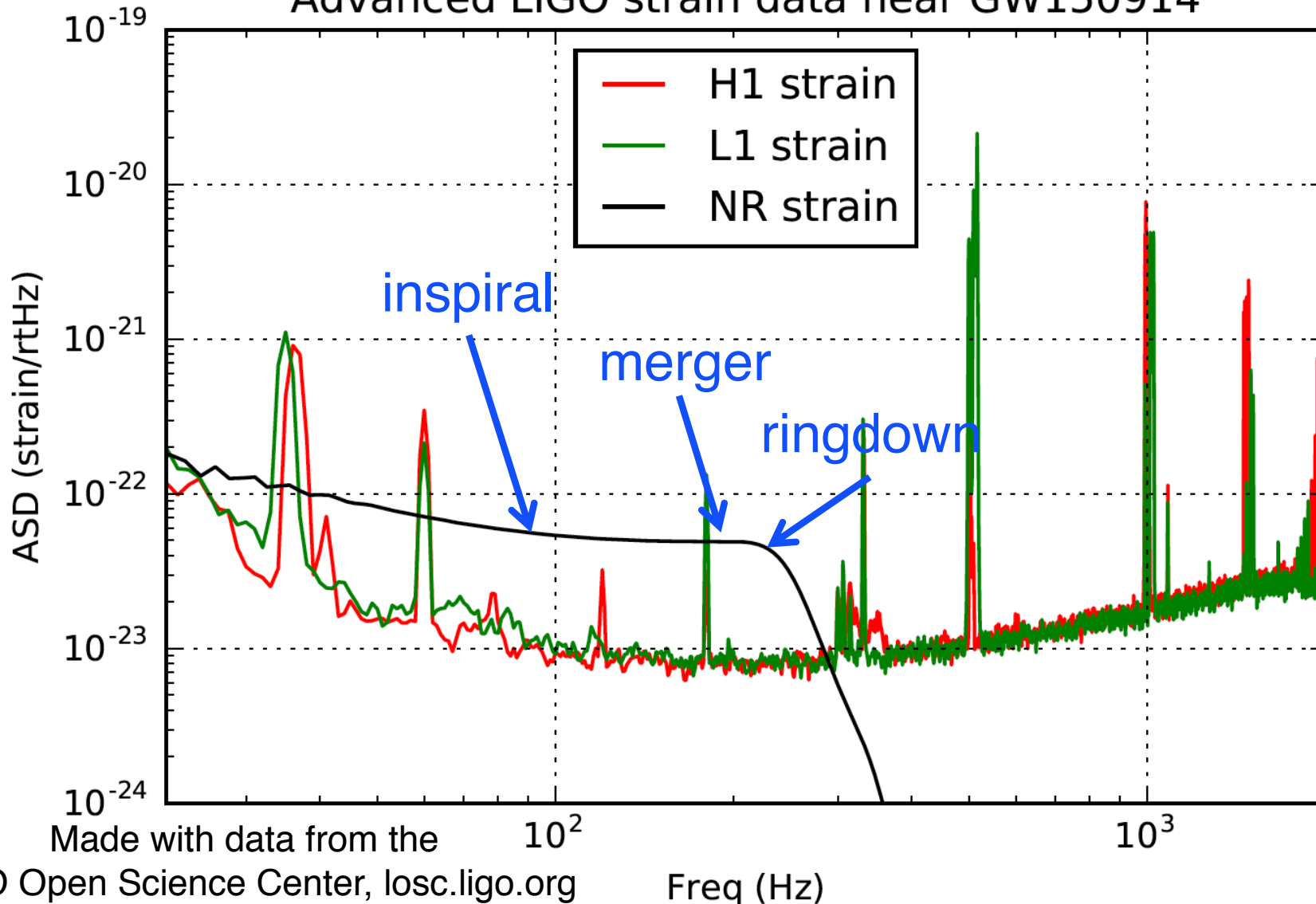
- filtered data
- freq-shifted data
- reconstructed & shifted



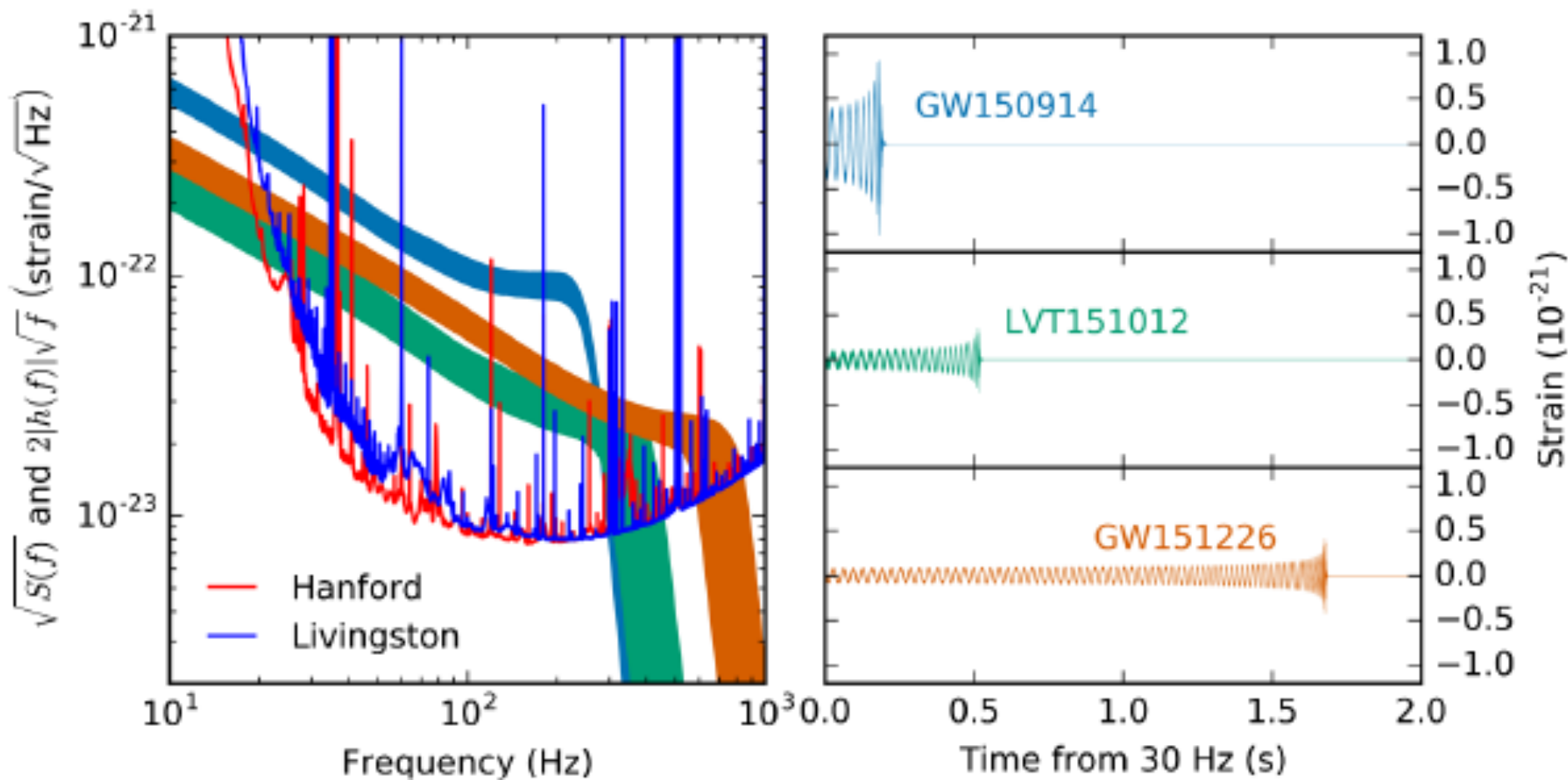
Whitened and band-passed [40-300] Hz

# GW150914 in the frequency domain

Advanced LIGO strain data near GW150914



# Three BBH events, compared



Abbott, et al., LIGO Scientific Collaboration and Virgo Collaboration, "Binary Black Hole Mergers in the first Advanced LIGO Observing Run", <https://arxiv.org/abs/1606.04856>, Phys. Rev. X 6, 041015 (2016)

# Exploring the Properties of GW150914

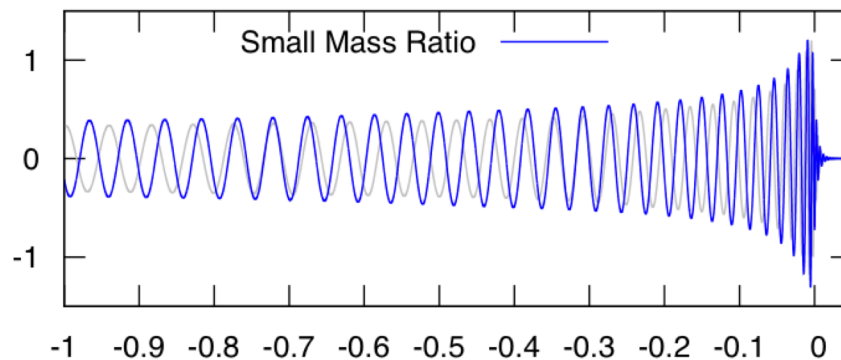
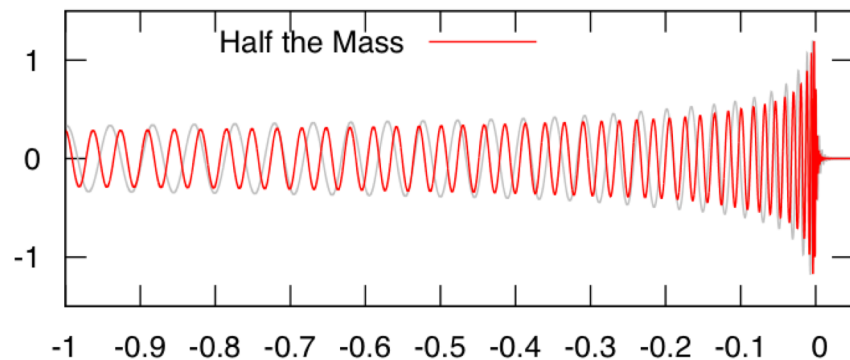
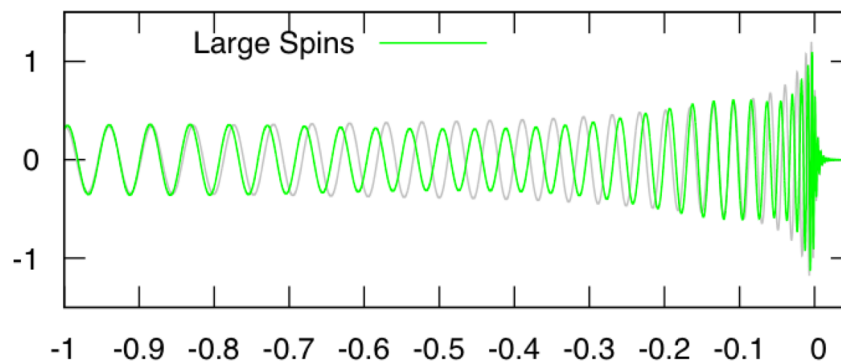
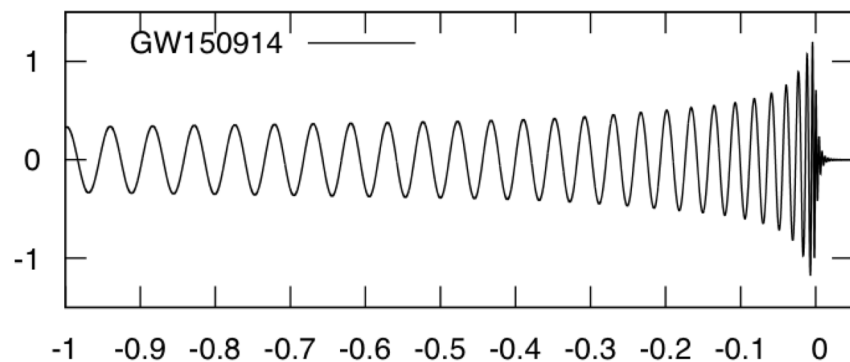


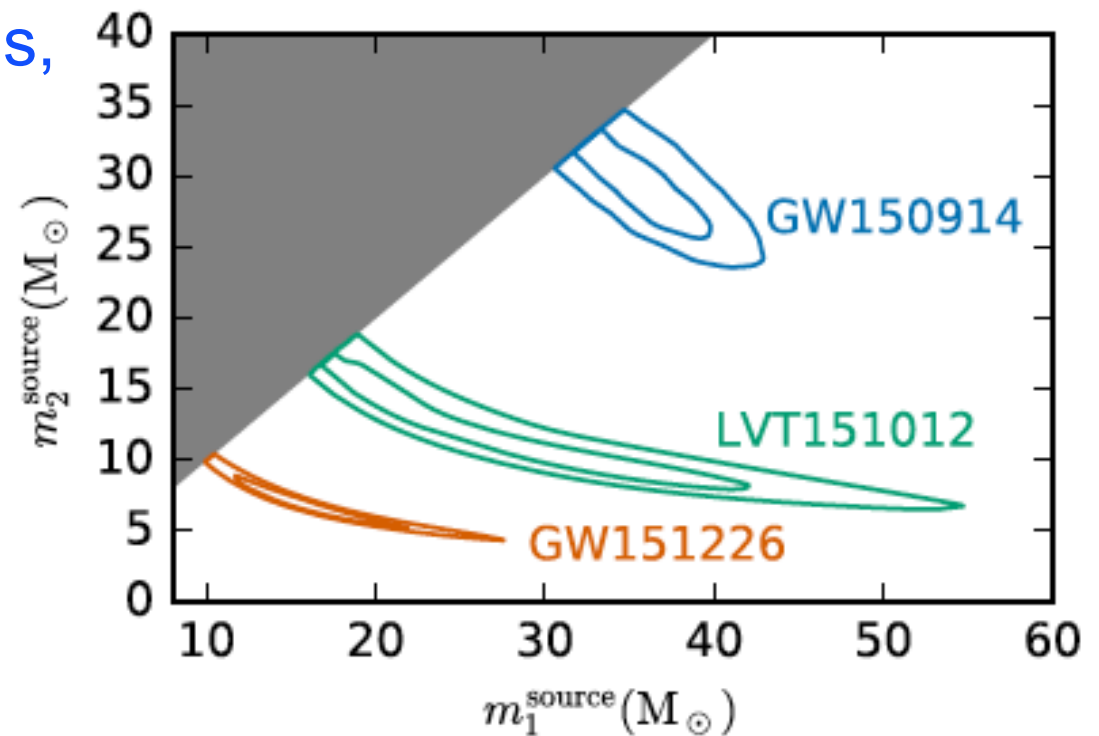
*Illustration by N. Cornish and T. Littenberg*

# Three BBH events, black hole masses

For the higher mass systems,  
we see the merger,  
measure  $M_{tot} = m_1 + m_2$

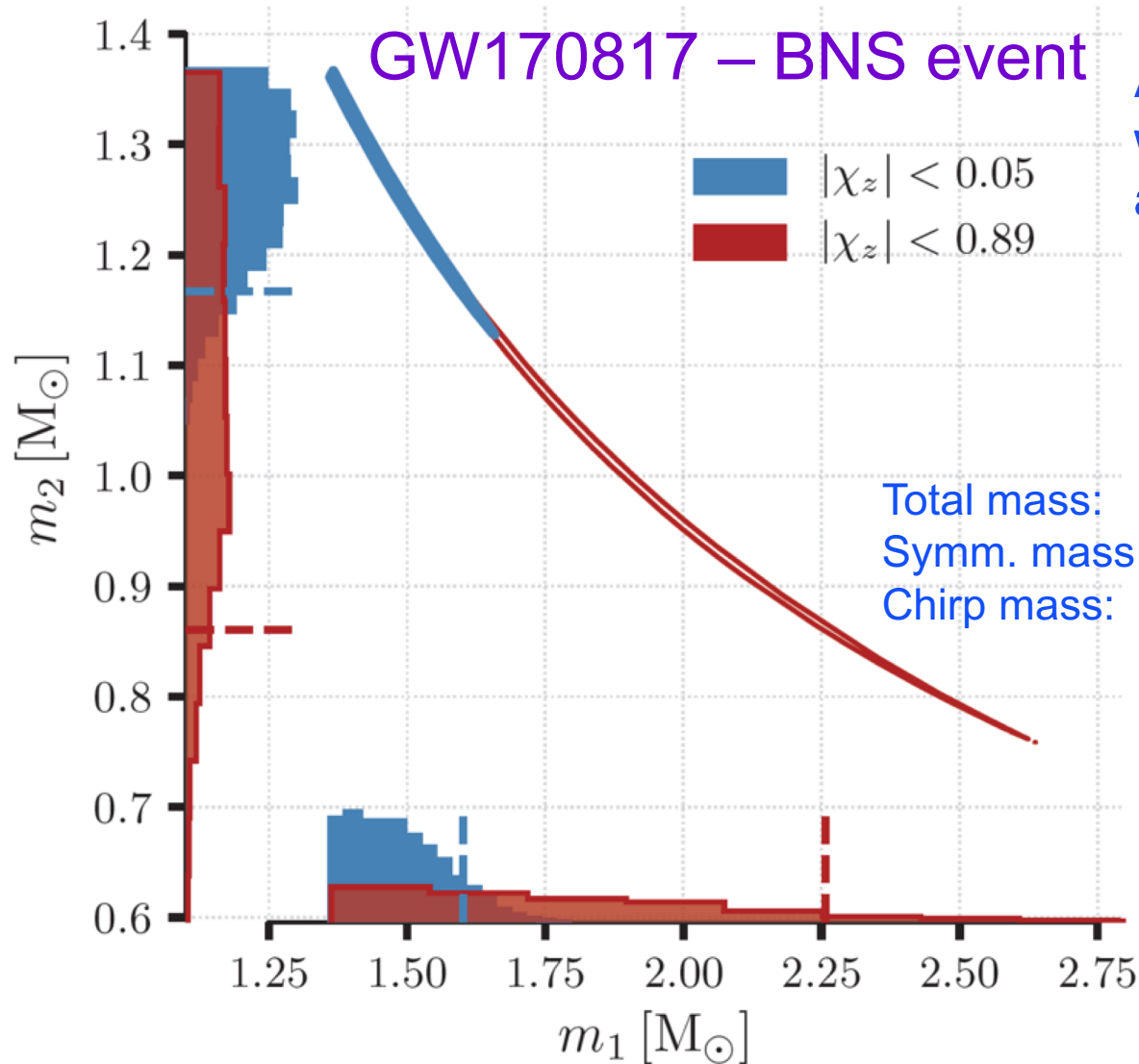
For lower mass systems,  
we see the inspiral,  
measure the “chirp mass”

$$\mathcal{M} = \frac{(m_1 m_2)^{3/5}}{M^{1/5}}$$



These masses are surprisingly large!

GWs measure the chirp mass best,  
the mass ratio less well.



And it depends on whether we think neutron stars spin a lot or only a little.

Total mass:

Symm. mass ratio:

Chirp mass:

$$M_{tot} = M_1 + M_2$$

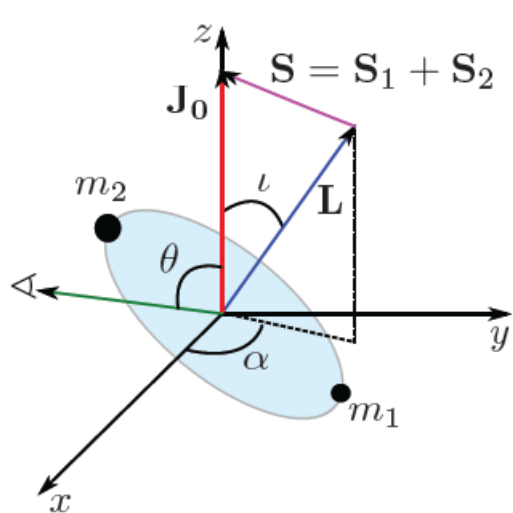
$$\eta = M_1 M_2 / M_{tot}^2$$

$$M_{ch} = M_{tot} \eta^{3/5}$$

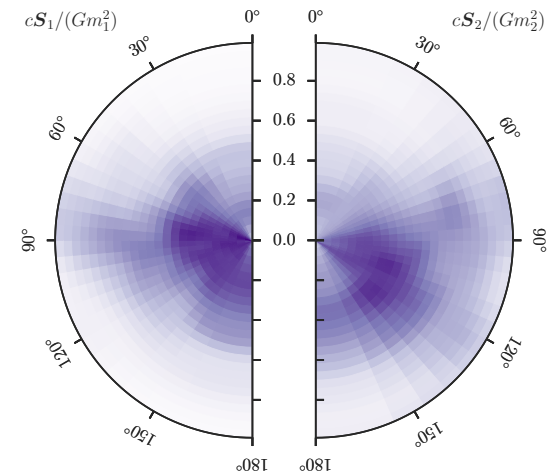
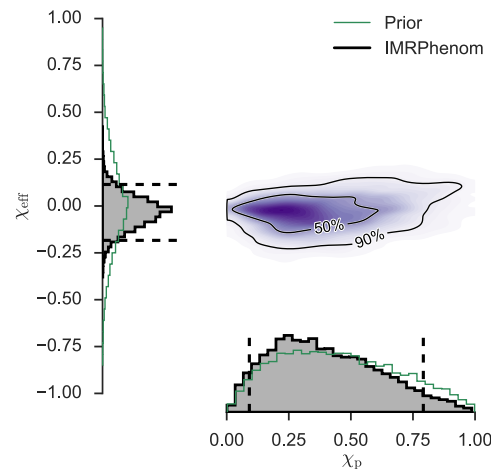
Assuming low spin, component masses are in the range 1.17 to 1.60  $M_\odot$ , typical of pulsars (NSs) in binaries

# BH spins – aligned with orbital angular momentum, and precessing spin

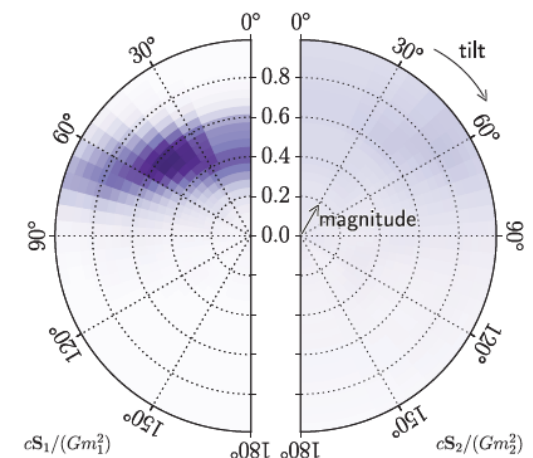
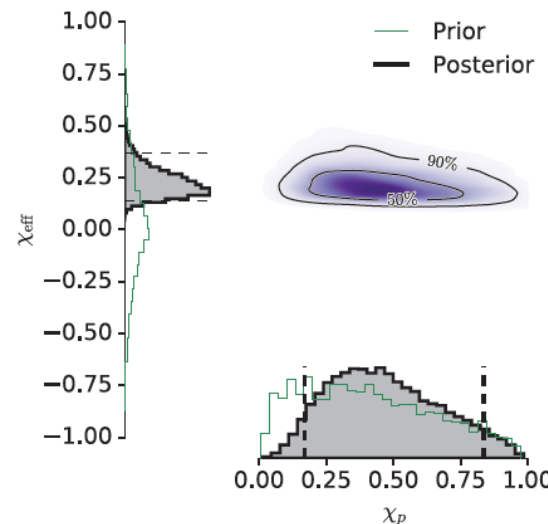
- The component BH spins measurably modulate the inspiral frequency evolution.
- Spin-orbit couplings cause the orbital plane to precess, producing amplitude modulation at the detectors.
- Parameterize with aligned spin  $\chi_{eff}$  and “precessing” spin  $\chi_P$



GW150914



GW151226



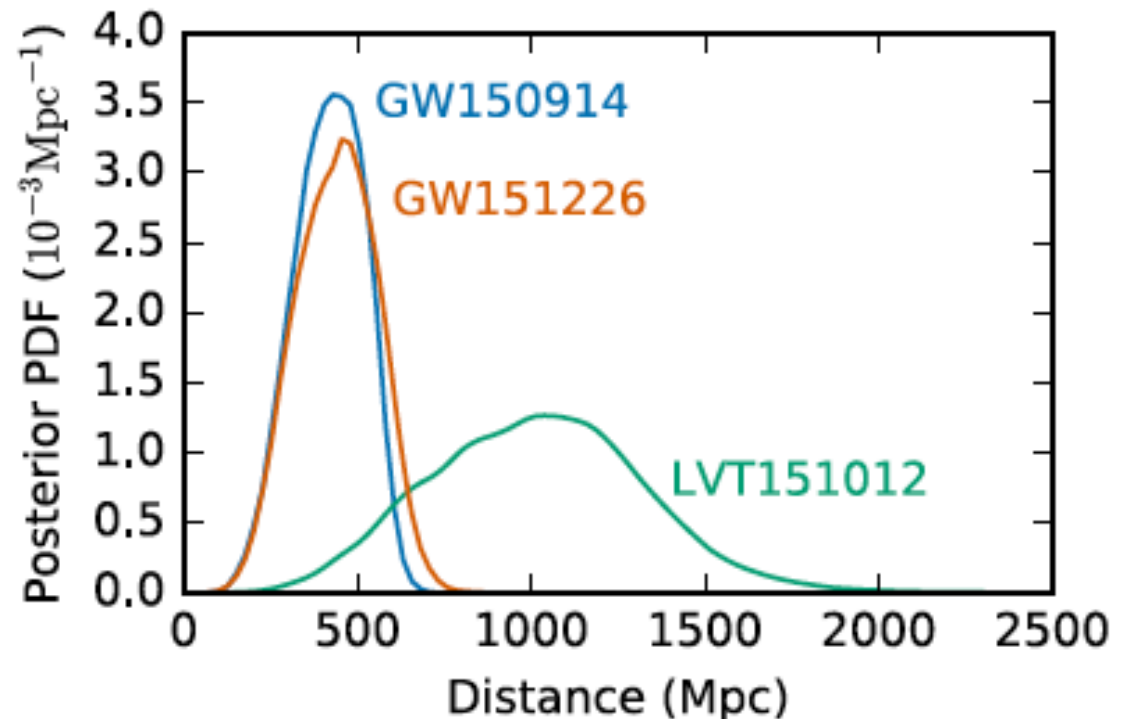
# Three BBH events, distances

It's hard to measure distances in astronomy!  
(few "standard candles")

BBH events are "standardizable sirens"  
(need to know their masses, orbital orientation, etc).

Distances measured poorly with only two detectors.

Our two loud events are far away!  
(400 Mpc ~ 1.3 Gly) – merged 1.3 By ago!





# Radiated energy & luminosity

▶ GW150914:

$$E_{\text{rad}} = 3.0^{+0.5}_{-0.4} M_{\odot} c^2$$

$$\ell_{\text{peak}} = 3.6^{+0.5}_{-0.4} \times 10^{56} \text{ erg/s}$$

▶ GW151226:

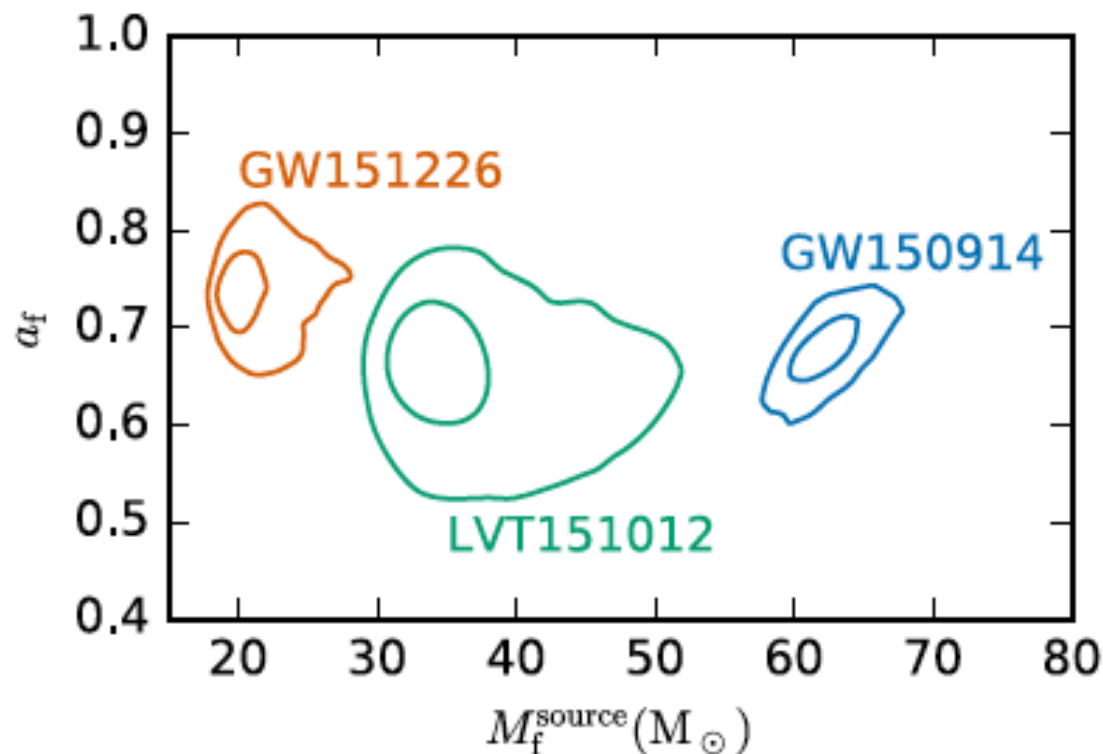
$$E_{\text{rad}} = 1.0^{+0.1}_{-0.2} M_{\odot} c^2$$

$$\ell_{\text{peak}} = 3.3^{+0.8}_{-1.6} \times 10^{56} \text{ erg/s}$$

▶ LVT151012:

$$E_{\text{rad}} = 1.5^{+0.3}_{-0.4} M_{\odot} c^2$$

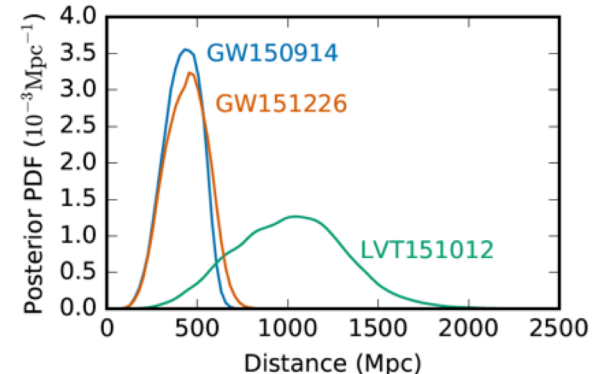
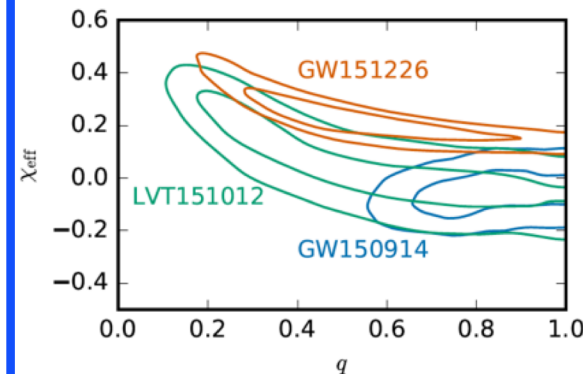
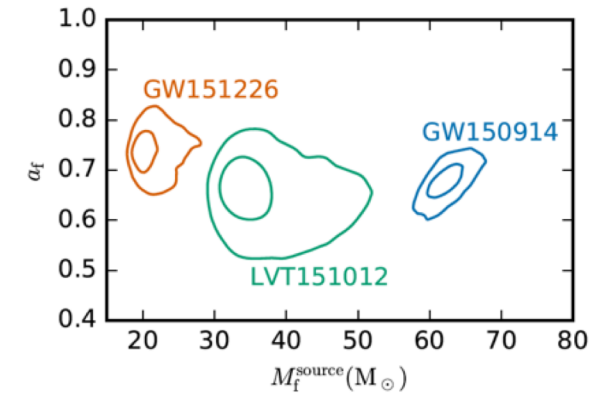
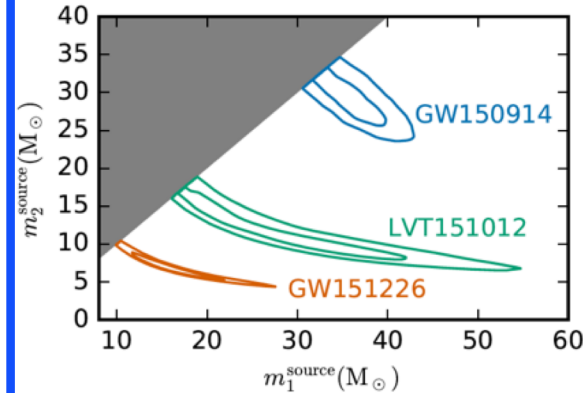
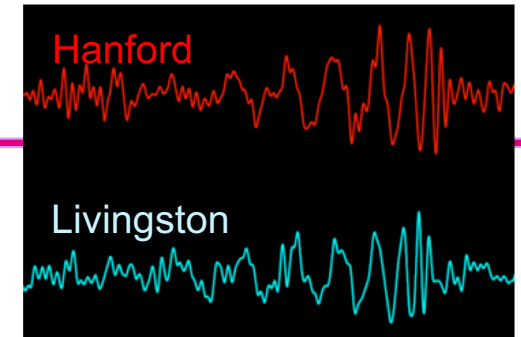
$$\ell_{\text{peak}} = 3.1^{+0.8}_{-1.8} \times 10^{56} \text{ erg/s}$$



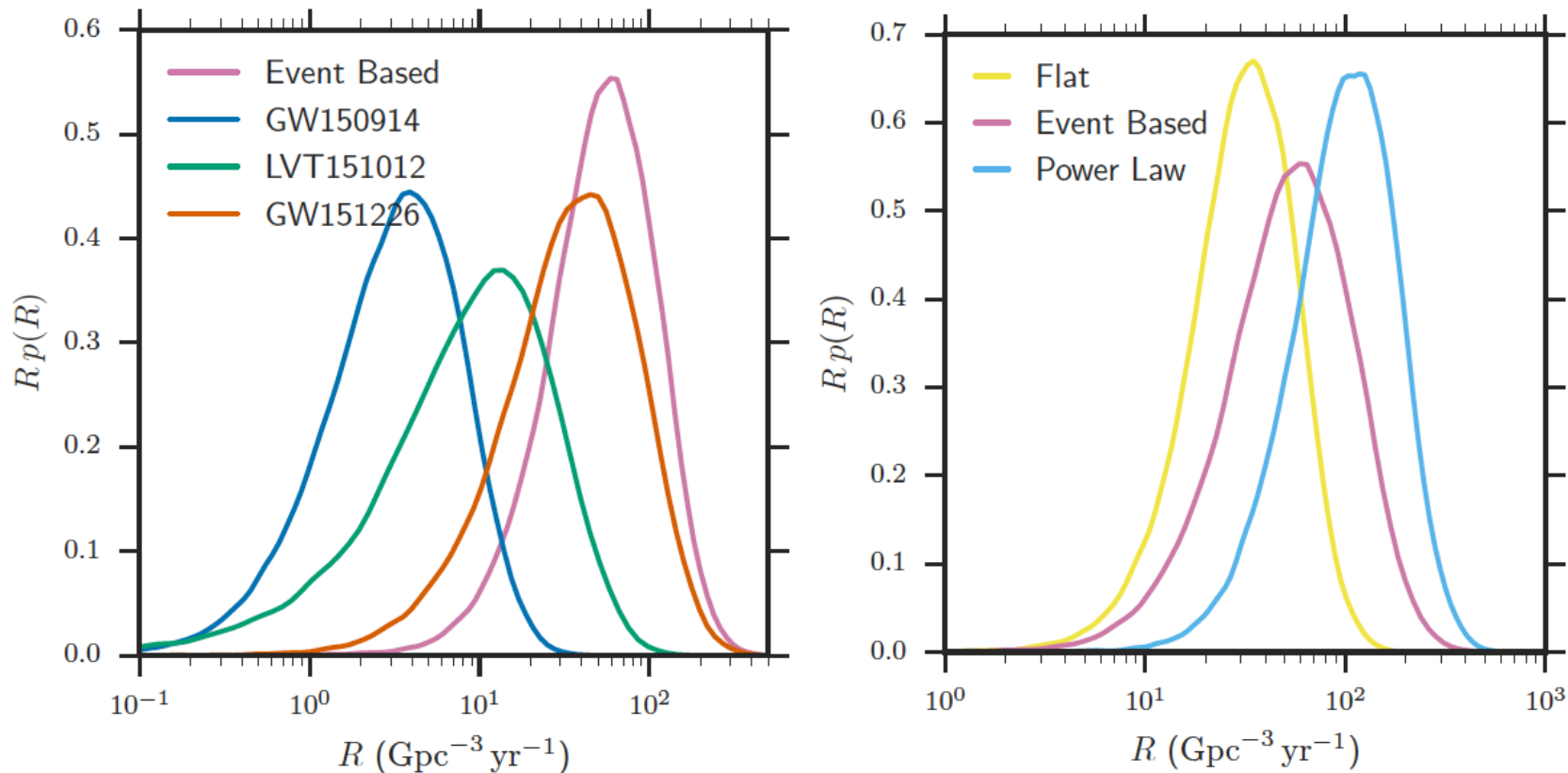
- GW150914:  $E_{\text{GW}} \approx 3 M_{\odot} c^2$ , or  $\sim 4.5\%$  of the total mass-energy of the system.
- Roughly  $10^{80}$  gravitons.
- Peak luminosity  $L_{\text{GW}} \sim 3.6 \times 10^{54} \text{ erg/s}$ , briefly outshining the EM energy output of all the stars in the observable universe (by a factor  $\sim 50$ ).

# Extracting Astrophysical Parameters from Detections

| Event                                                    | GW150914                           | GW151226                           | LVT151012                          |
|----------------------------------------------------------|------------------------------------|------------------------------------|------------------------------------|
| Signal-to-noise ratio $\rho$                             | 23.7                               | 13.0                               | 9.7                                |
| False alarm rate FAR/yr <sup>-1</sup>                    | $< 6.0 \times 10^{-7}$             | $< 6.0 \times 10^{-7}$             | 0.37                               |
| p-value                                                  | $7.5 \times 10^{-8}$               | $7.5 \times 10^{-8}$               | 0.045                              |
| Significance                                             | $> 5.3\sigma$                      | $> 5.3\sigma$                      | $1.7\sigma$                        |
| Primary mass $m_1^{\text{source}}/M_\odot$               | $36.2^{+5.2}_{-3.8}$               | $14.2^{+8.3}_{-3.7}$               | $23^{+18}_{-6}$                    |
| Secondary mass $m_2^{\text{source}}/M_\odot$             | $29.1^{+3.7}_{-4.4}$               | $7.5^{+2.3}_{-2.3}$                | $13^{+4}_{-5}$                     |
| Chirp mass $\mathcal{M}^{\text{source}}/M_\odot$         | $28.1^{+1.8}_{-1.5}$               | $8.9^{+0.3}_{-0.3}$                | $15.1^{+1.4}_{-1.1}$               |
| Total mass $M^{\text{source}}/M_\odot$                   | $65.3^{+4.1}_{-3.4}$               | $21.8^{+5.9}_{-1.7}$               | $37^{+13}_{-4}$                    |
| Effective inspiral spin $\chi_{\text{eff}}$              | $-0.06^{+0.14}_{-0.14}$            | $0.21^{+0.20}_{-0.10}$             | $0.0^{+0.3}_{-0.2}$                |
| Final mass $M_f^{\text{source}}/M_\odot$                 | $62.3^{+3.7}_{-3.1}$               | $20.8^{+6.1}_{-1.7}$               | $35^{+14}_{-4}$                    |
| Final spin $a_f$                                         | $0.68^{+0.05}_{-0.06}$             | $0.74^{+0.06}_{-0.06}$             | $0.66^{+0.09}_{-0.10}$             |
| Radiated energy $E_{\text{rad}}/(M_\odot c^2)$           | $3.0^{+0.5}_{-0.4}$                | $1.0^{+0.1}_{-0.2}$                | $1.5^{+0.3}_{-0.4}$                |
| Peak luminosity $\ell_{\text{peak}}/(\text{erg s}^{-1})$ | $3.6^{+0.5}_{-0.4} \times 10^{56}$ | $3.3^{+0.8}_{-1.6} \times 10^{56}$ | $3.1^{+0.8}_{-1.8} \times 10^{56}$ |
| Luminosity distance $D_L/\text{Mpc}$                     | $420^{+150}_{-180}$                | $440^{+180}_{-190}$                | $1000^{+500}_{-500}$               |
| Source redshift $z$                                      | $0.09^{+0.03}_{-0.04}$             | $0.09^{+0.03}_{-0.04}$             | $0.20^{+0.09}_{-0.09}$             |
| Sky localization $\Delta\Omega/\text{deg}^2$             | 230                                | 850                                | 1600                               |



# Astrophysical rates

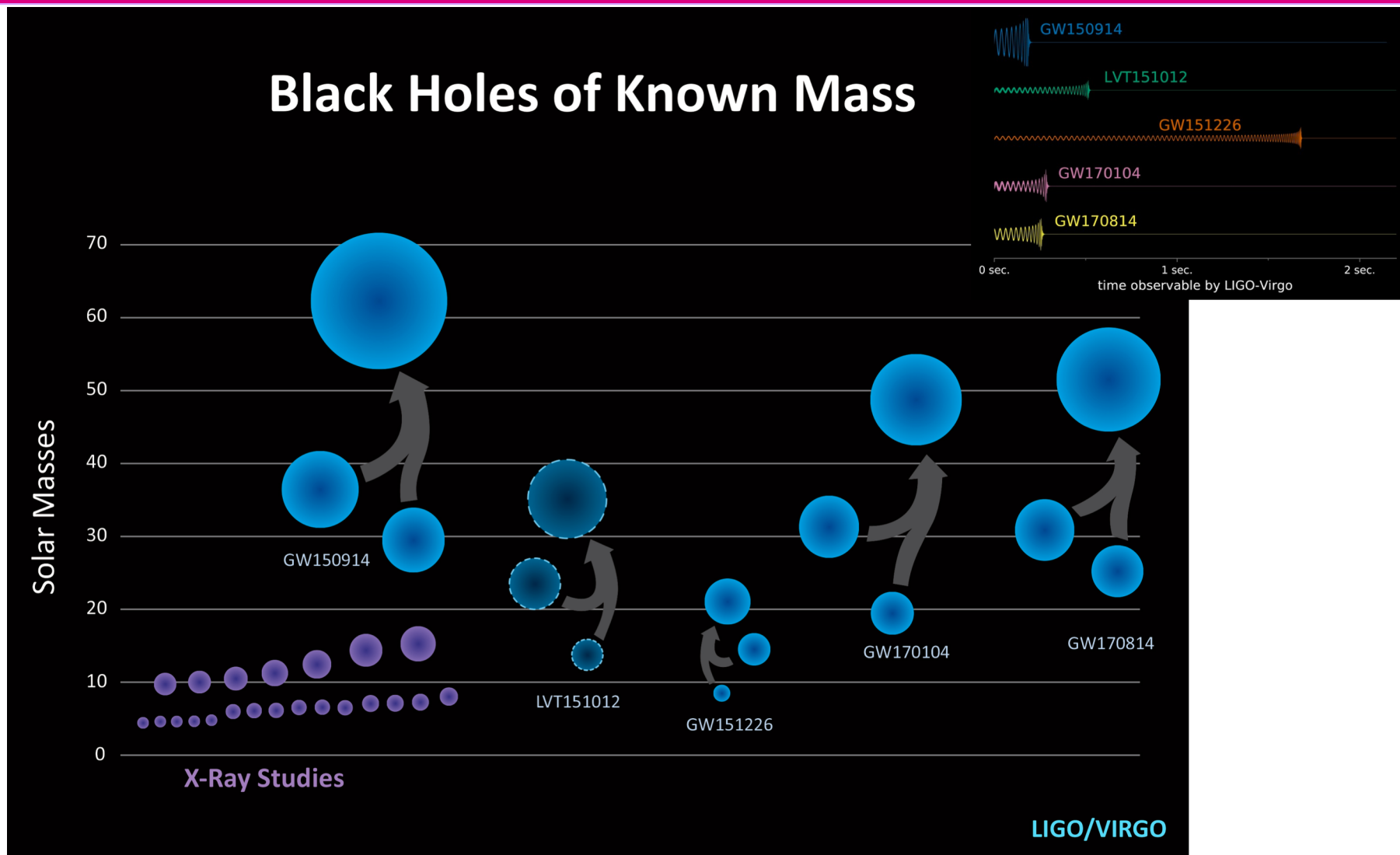


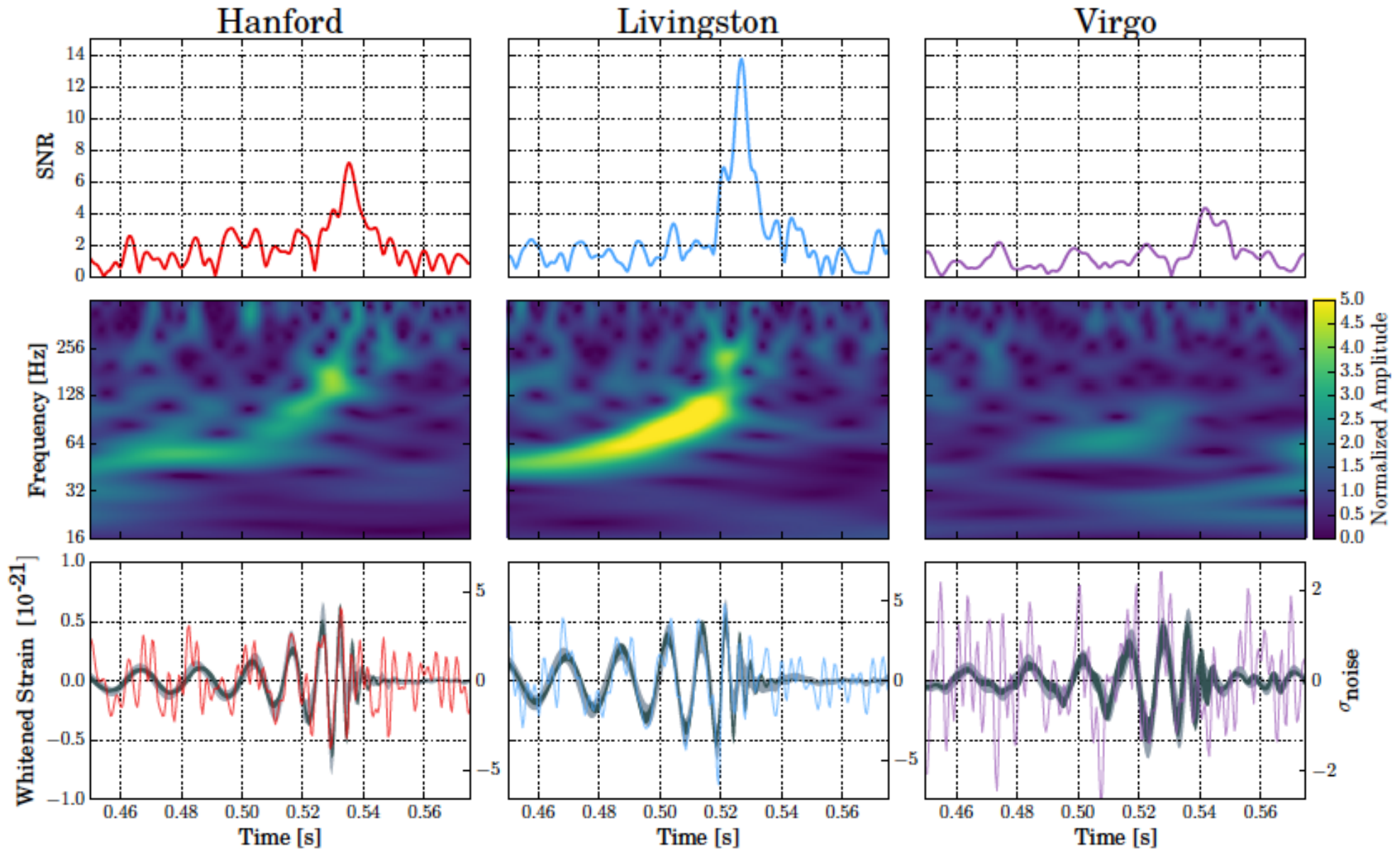
Roughly consistent with astrophysical expectations from:

- Core collapse supernova rate
- Short GRB rate
- Astrophysical modeling of compact binary formation (“population synthesis”)
- A half-dozen BNS systems in our galaxy (including Hulse-Taylor)

# MORE BBHs, in O2.

## Starting to build up a mass distribution



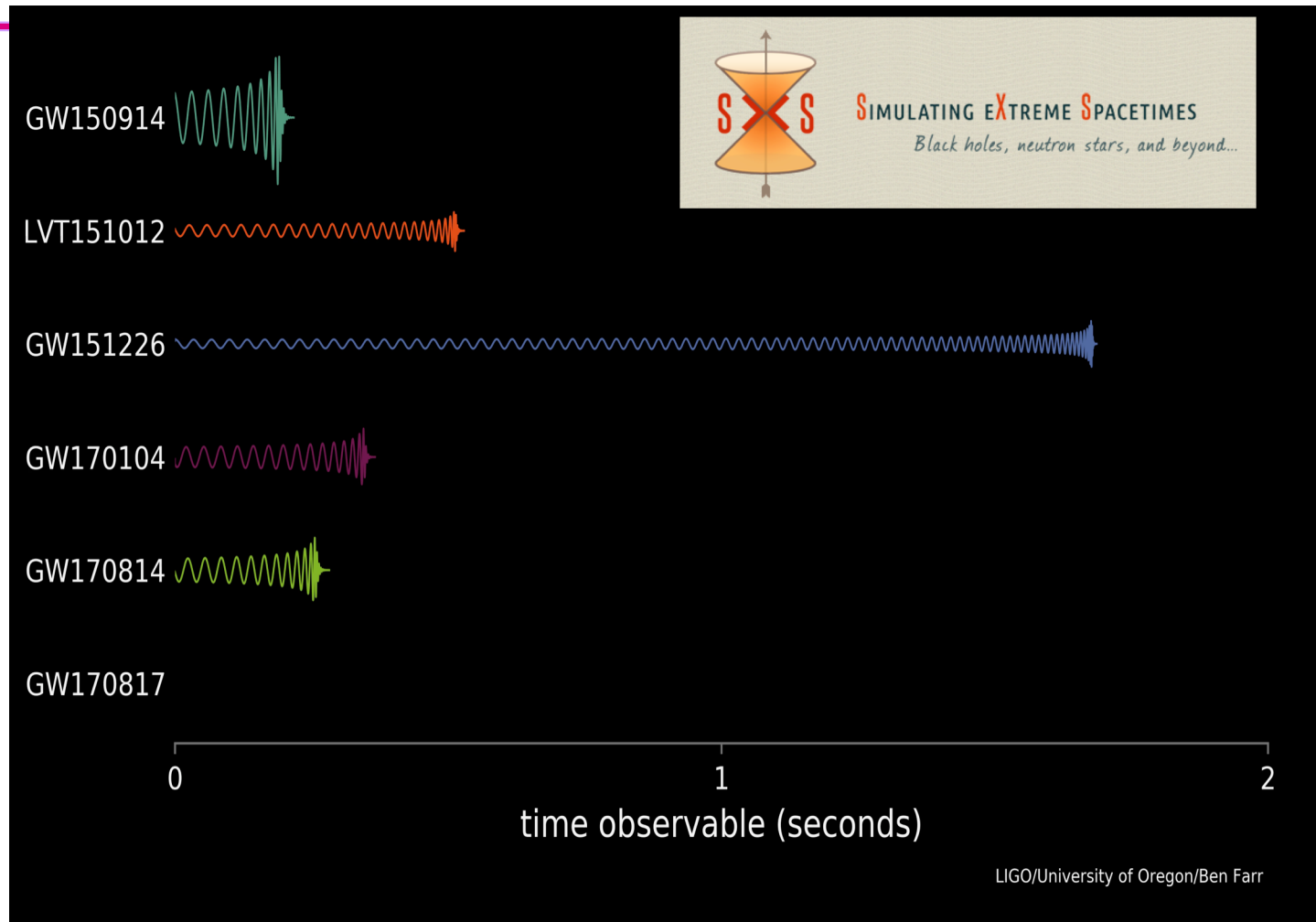




# Our automated software (“pipeline”) matched the GW signal



## to a predicted waveform for a binary neutron star merger



**The longest (~ 60 s), loudest (SNR ~ 32), closest (40 Mpc) signal LIGO has ever observed!**

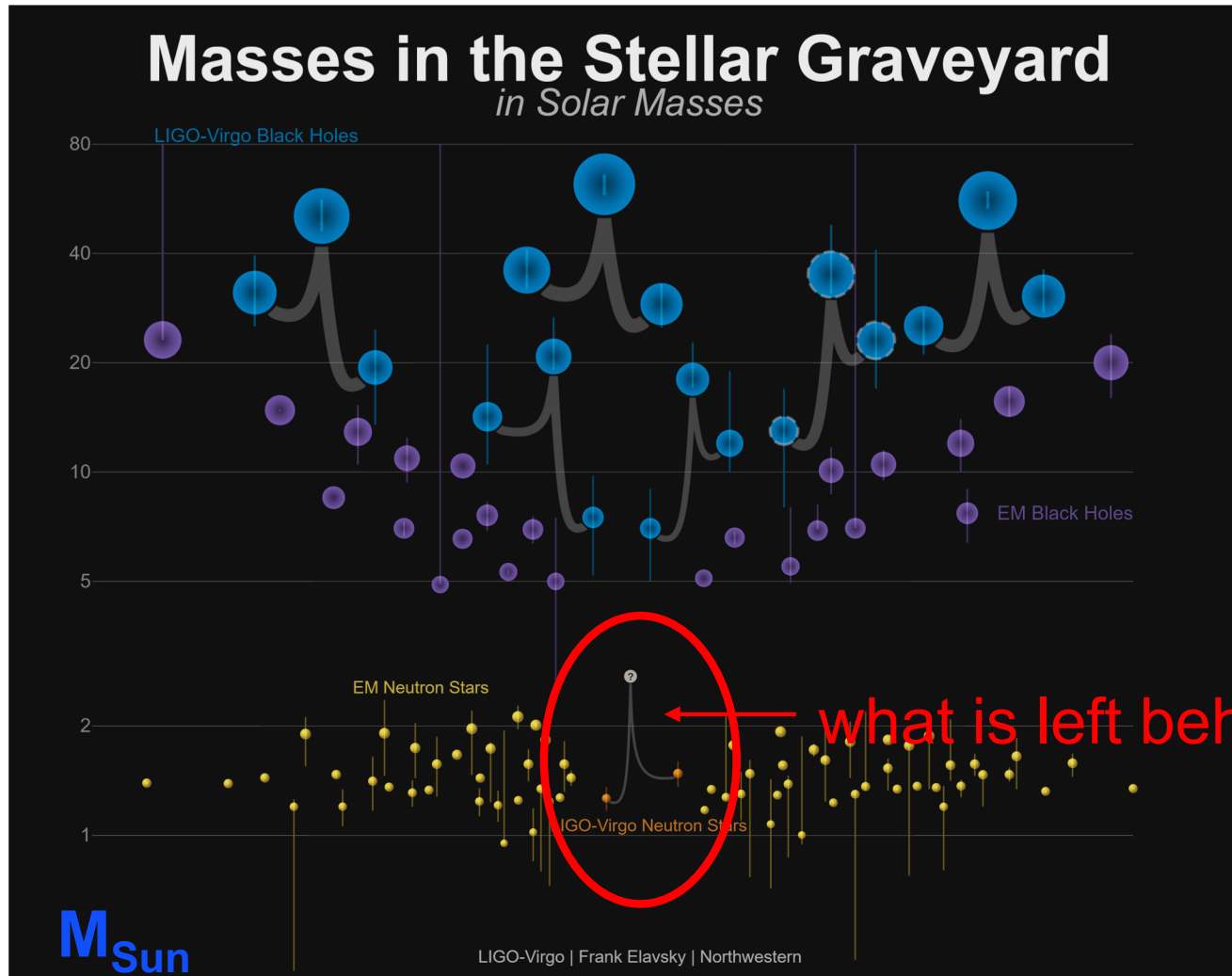
<https://www.youtube.com/watch?v=WoDCPTLgXH4>



**LIGO**



We can measure the masses  
(in the combination “Chirp mass”) very well:



“stellar mass”  
black holes

“mass gap”?

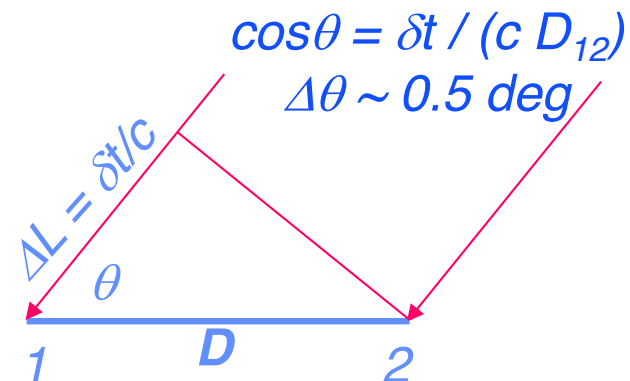
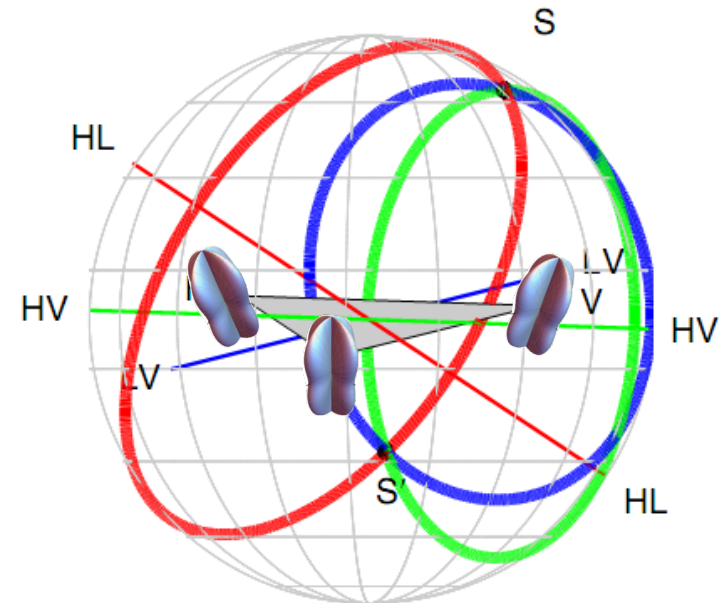
Neutron stars  
(pulsars)

what is left behind?

<http://ligo.org/detections/GW170817.php>

# Event Localization With An Array of GW Interferometers

- Gravitational-wave astronomy is *greatly* enhanced by having a multiplicity of interferometers distributed over the globe.
  - » GW interferometry, ‘Aperture synthesis’
- Advantages include:
  - » Source localization *in near real time*
  - » Enhanced network sky coverage
  - » Maximum time coverage – a fraction of the detectors are ‘always listening’
  - » Detection confidence - coincidence
  - » Source parameter estimation
  - » Polarization resolution



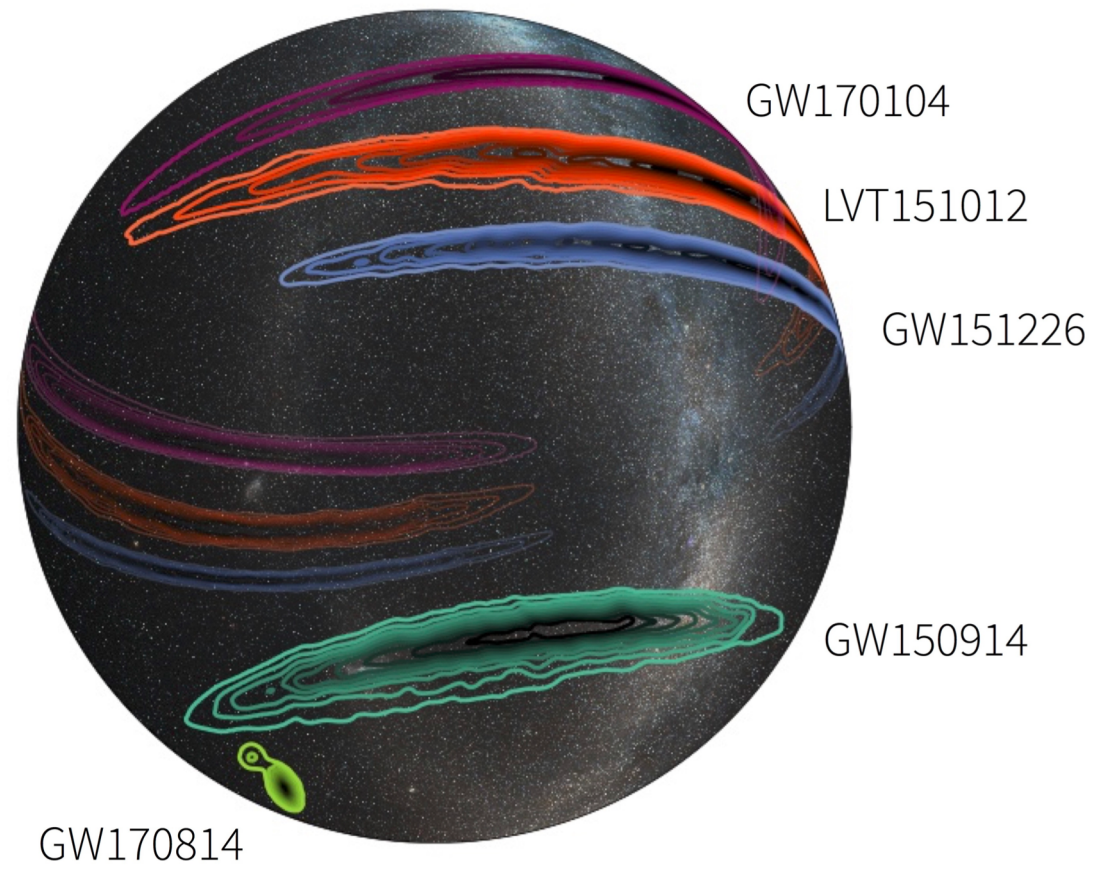
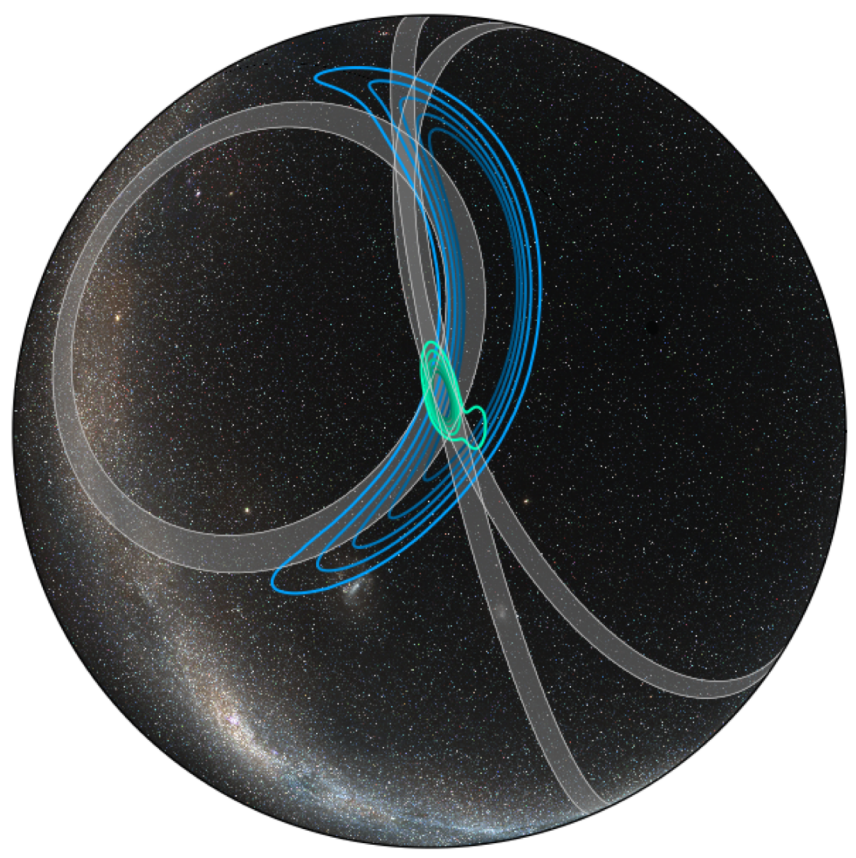




**LIGO**



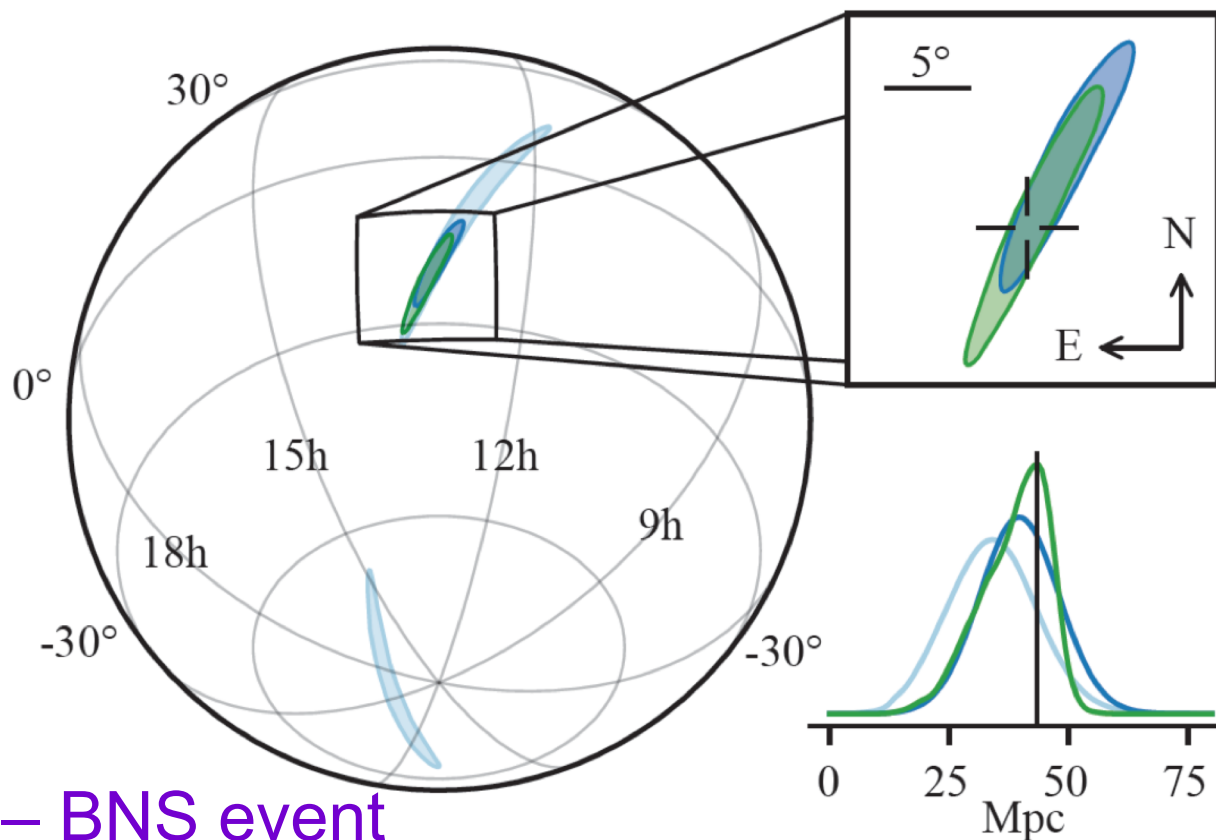
# Greatly improved sky localization (but, these are black holes...)



Credit: LIGO/Virgo/NASA/Leo Singer (Milky Way image: Axel Mellinger)

<http://ligo.org/detections/GW170814.php>

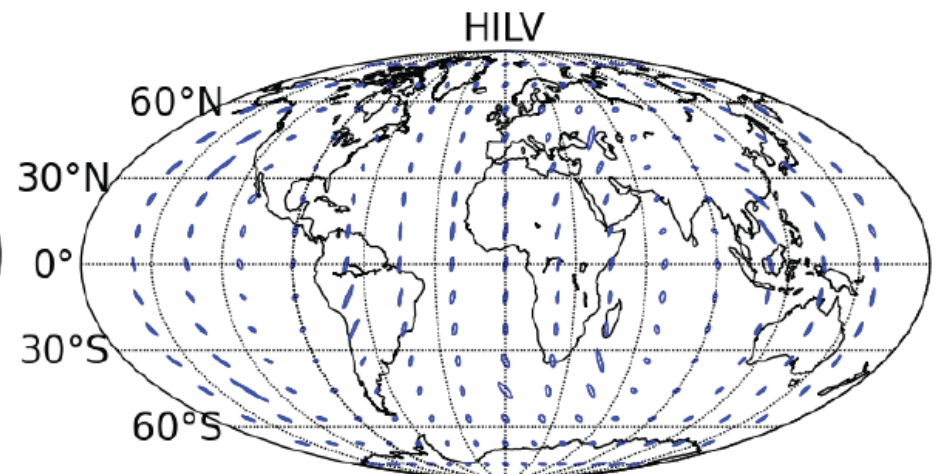
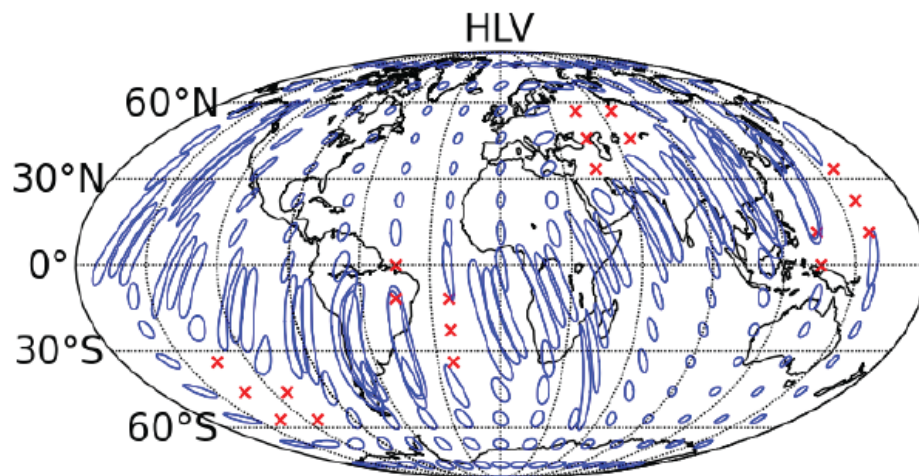
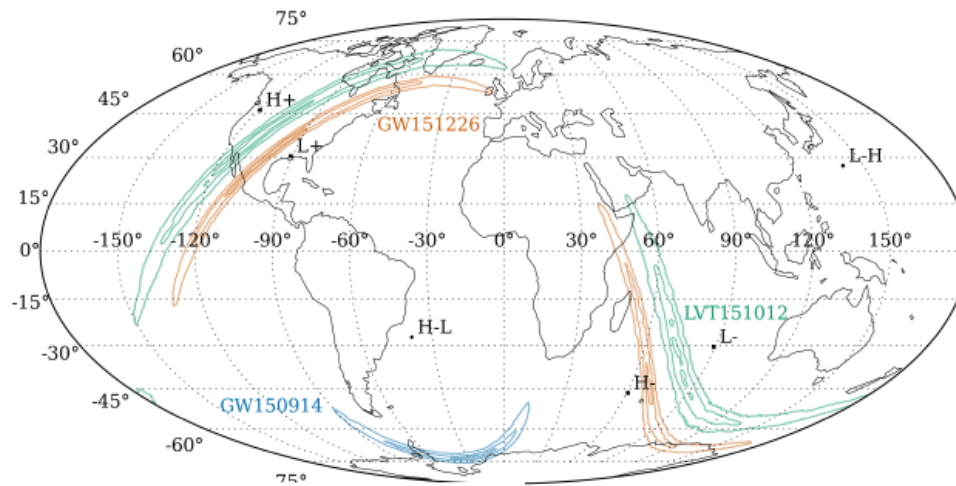
# 3-dimensional localization



## GW170817 – BNS event

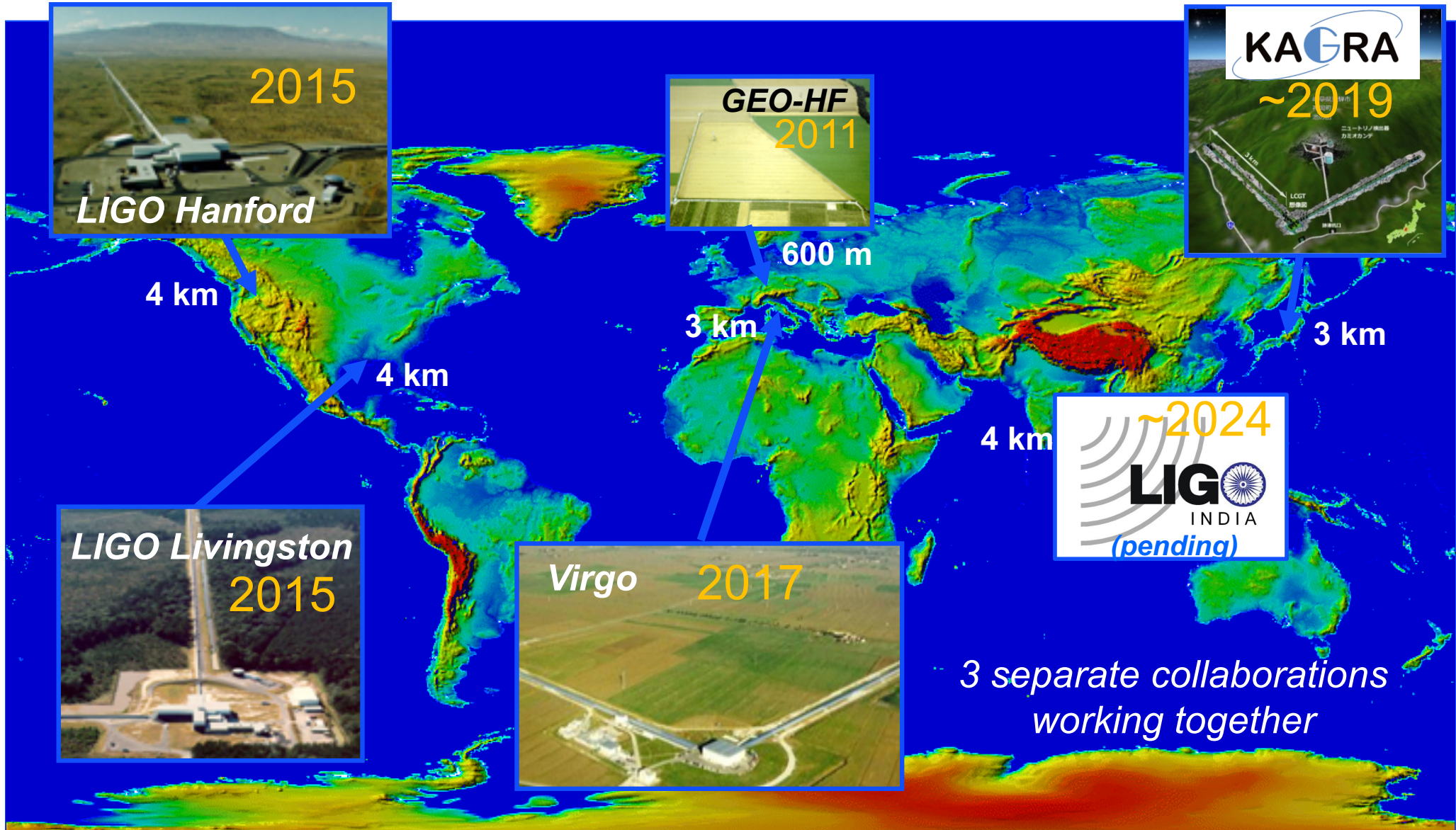
The source was localized within a sky region of  $28 \text{ deg}^2$  (90% probability) and had a luminosity distance of  $40_{-14}^{+8} \text{ Mpc}$ , the closest and most precisely localized gravitational-wave signal

# Source localization with the global network of GW detectors



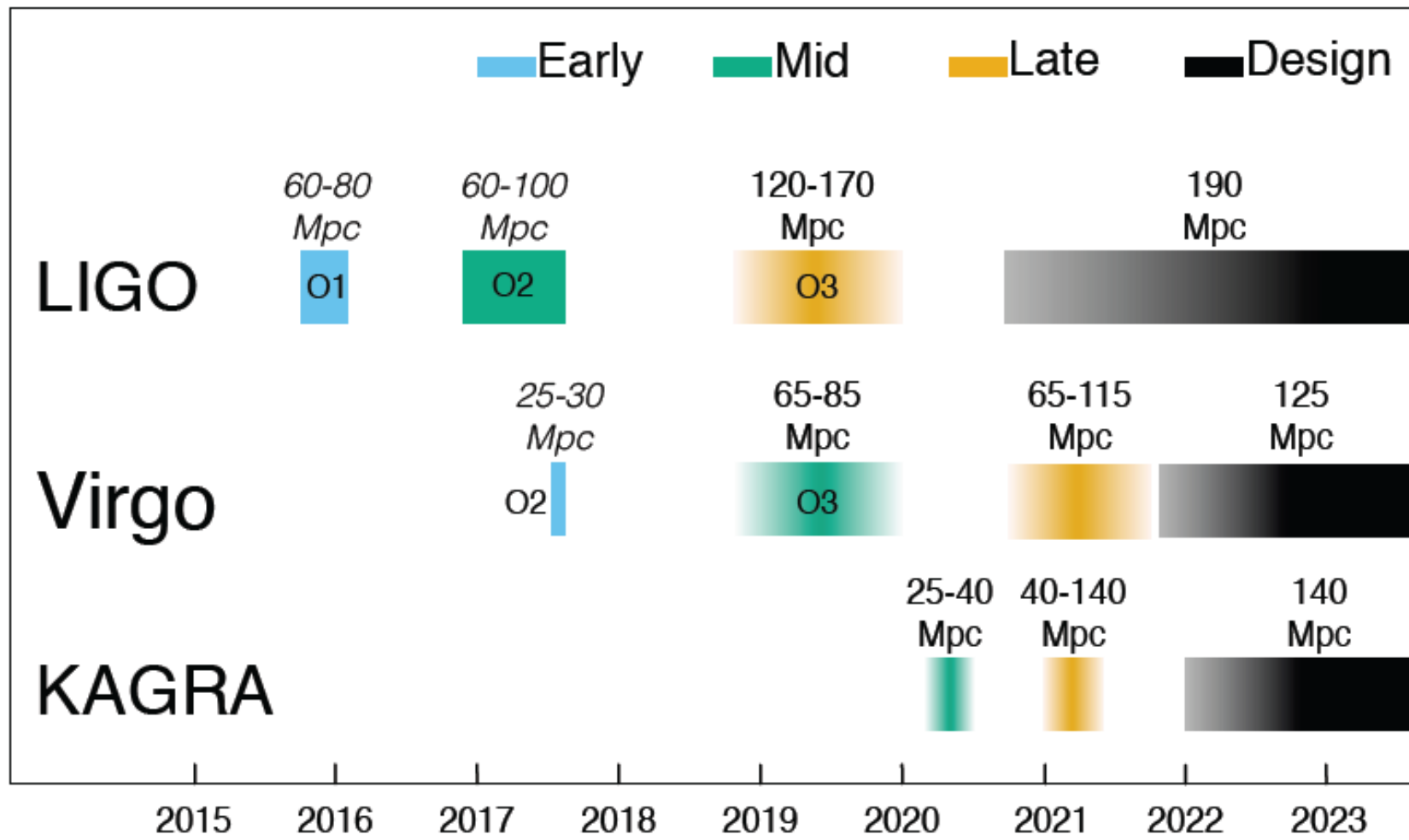


# The emerging Advanced GW Detector Network



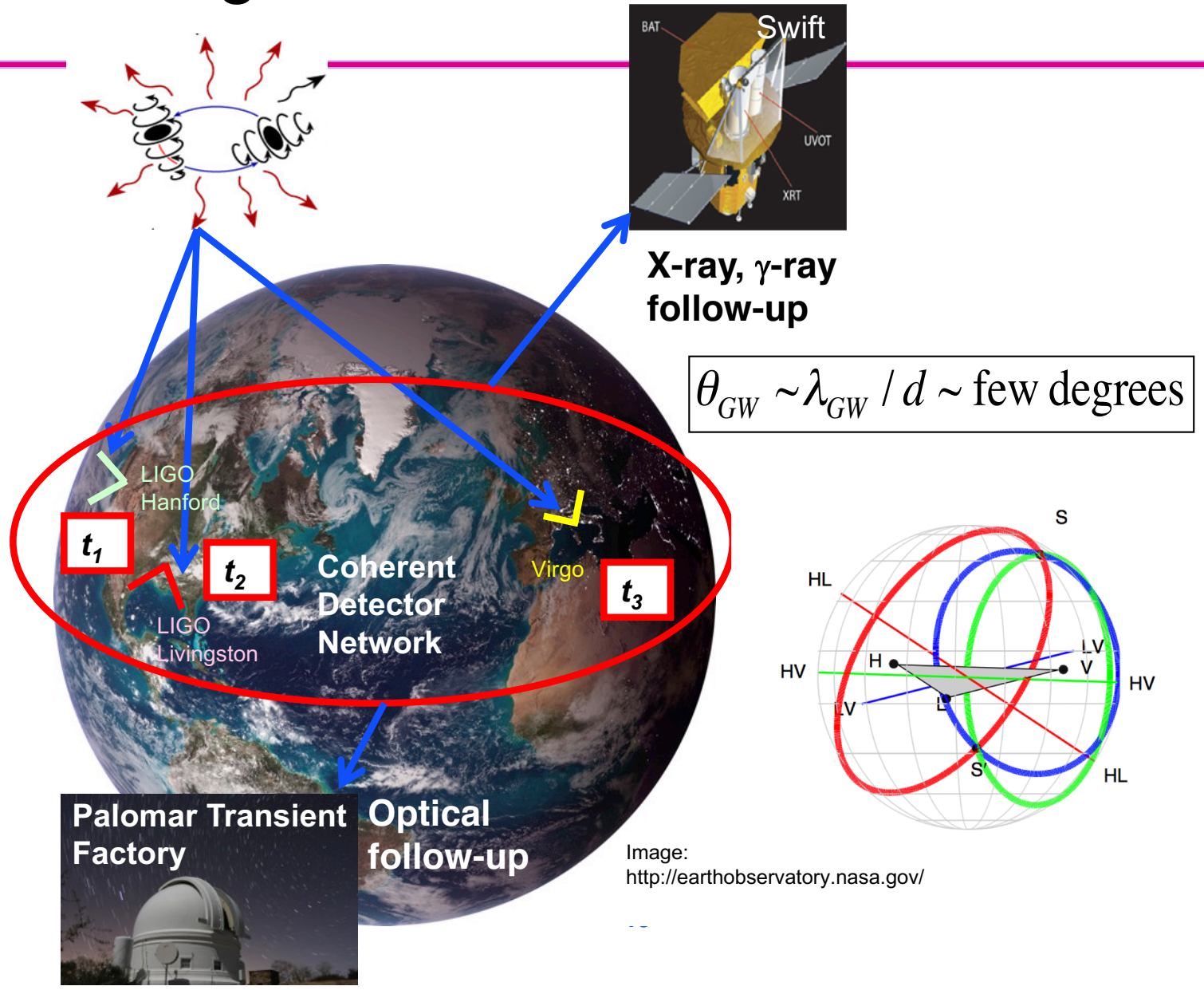
3 separate collaborations working together

# Coming years: more, and more sensitive detectors



<https://arxiv.org/abs/1304.0670>

# LIGO Enabling multi-messenger astronomy with gravitational waves

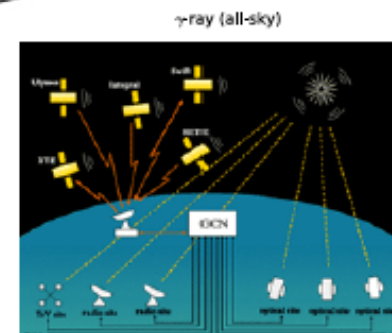
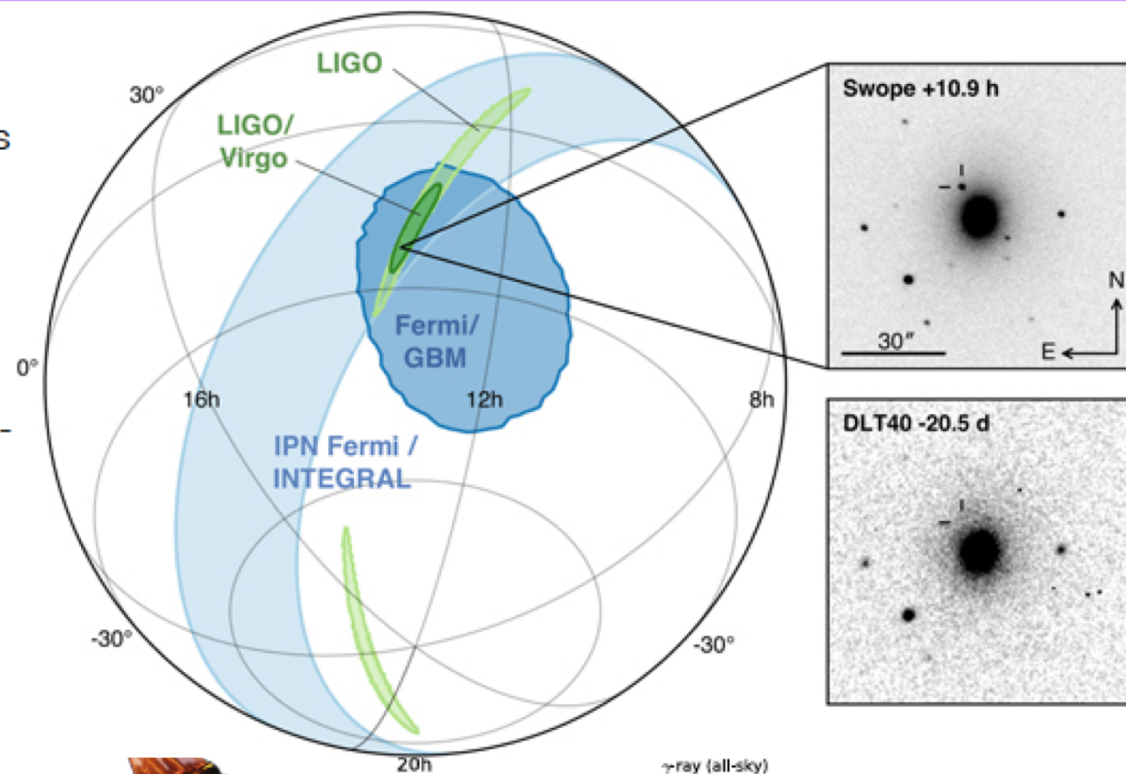


Abadie, et al, (LSC & Virgo Collaborations)  
 Astron. Astrophys. **541** (2012) A155.  
 Nissanke, Kalsiwal, Georgieva,  
 Astrophysical J. **767** (2013) 124.  
 Singer, Price, et al., Astrophysical J., 795  
 (2014) 105.

Image:  
<http://earthobservatory.nasa.gov/>

# Localization and broadband follow-up of BNS event GW170817

- Consortium between LIGO and 63 teams using ground and space facilities
- Gamma-ray, X-ray, optical, infrared, and radio wavelengths
- Key NASA contributions come from high-energy observational assets: **Fermi**, **Swift**, **GCN network**



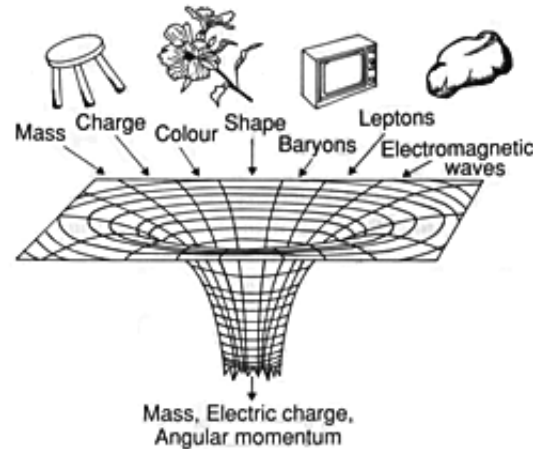
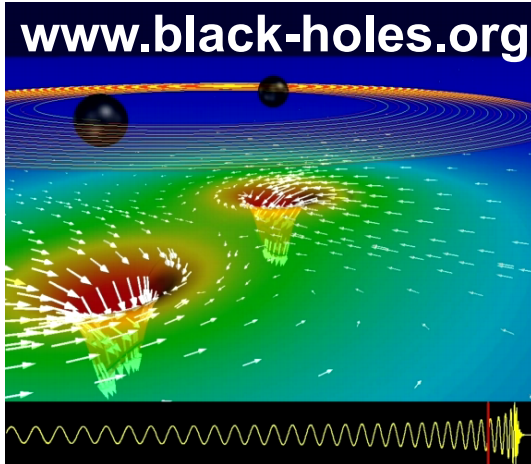
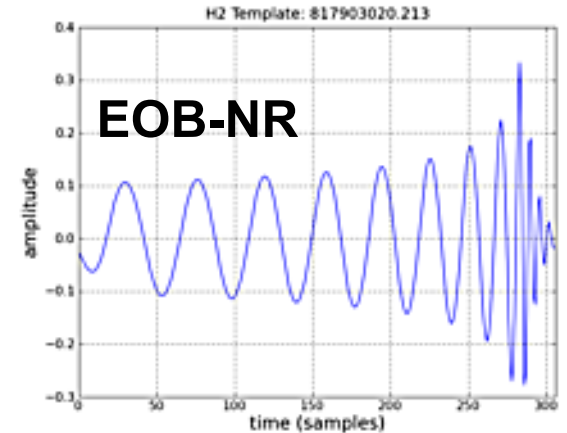
*Multi-messenger Observations of a Binary Neutron Star Merger*, *Astrophys. J. Lett.* 848:L12 (2017)

# Testing General Relativity in the strong-field, dynamical regime

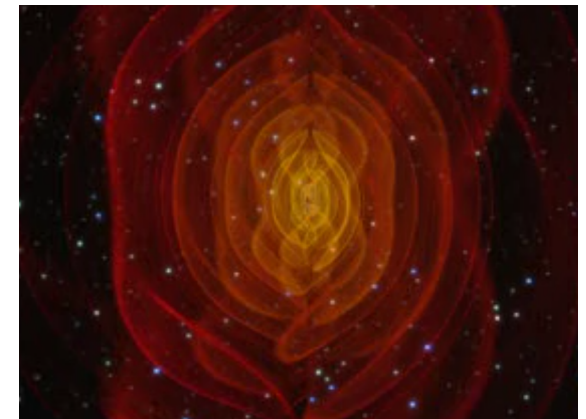
- Test post-Newtonian expansion of inspiral phase.

$$\Psi(f) \equiv 2\pi f t_0 + \varphi_0 + \frac{3}{128\eta v^5} \left( 1 + \sum_{k=2}^7 v^k \psi_k \right).$$

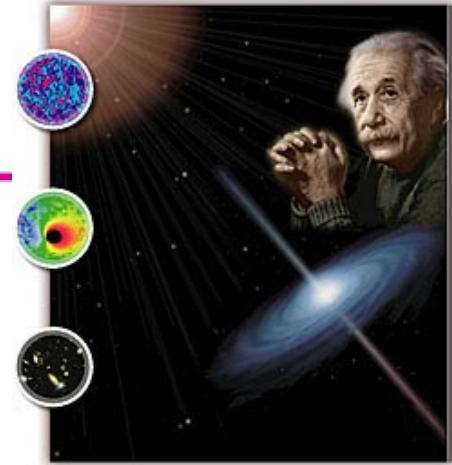
- Test Numerical Relativity waveform prediction for merger phase.
- Test association of inspiral and ringdown phases: BH perturbation theory, no-hair theorem.



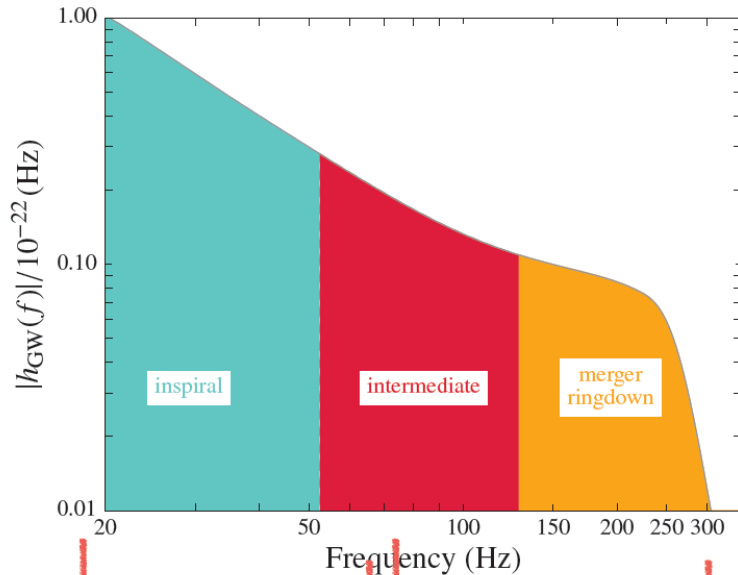
nonlocal.com/hbar/blackholes.html





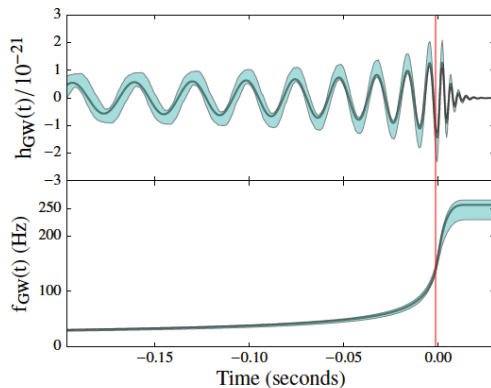


- **We can test GR in the new regime of strong-field, highly dynamical gravity!**
- **Gravitational lensing & multiple “images” (not beyond GR!)**
- **Constrain “parameterized post-Einsteinian framework” (Yunes & Pretorius, 2009)**
- **Directly measure speed of gravitational waves ( $c_{\text{GW}} \neq c_{\text{light}}$ ), constrain (or measure) the mass of the graviton.**
- **Constrain (or measure) longitudinal (vector, scalar) polarizations.**
- **Constrain (or measure) Lorentz violating effects.**
- **Constrain (or measure) cosmic anisotropies.**
- **Constrain (or measure) parity-violating effects.**
- **Constrain (or measure) dissipative gravity effects.**
- **Test specifically for scalar-tensor and other alt-gravity theories**
- **Quantum Gravity: echoes from “firewalls”, ...**



Post-Newtonian theory

Calibration on numerical solutions



- Waveform models are described by post-Newtonian and phenomenological coefficients calibrated against numerical relativity (NR) solutions

$$h(f) = A(f)e^{i\Phi(f)}$$

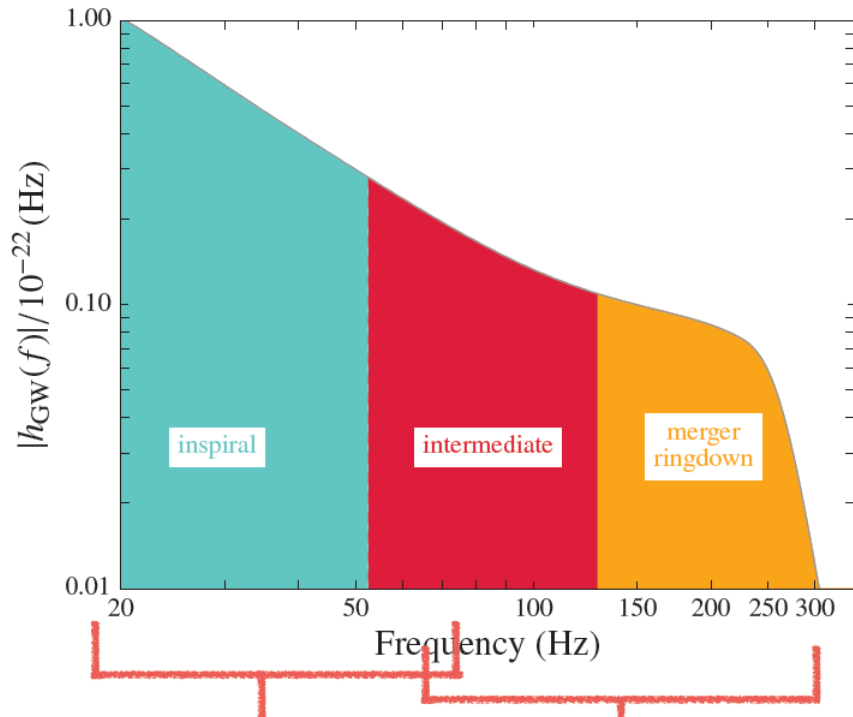
$$\Phi(f) = \sum_{k=1}^7 (\varphi_k + \varphi_k^l \log(f)) f^{(5-k)/3} + \sum_{i \neq k} \varphi_i f^i$$

$$\varphi_j \equiv \varphi_j(m_1, m_2, \vec{s}_1, \vec{s}_2) \quad \forall j = k, i$$

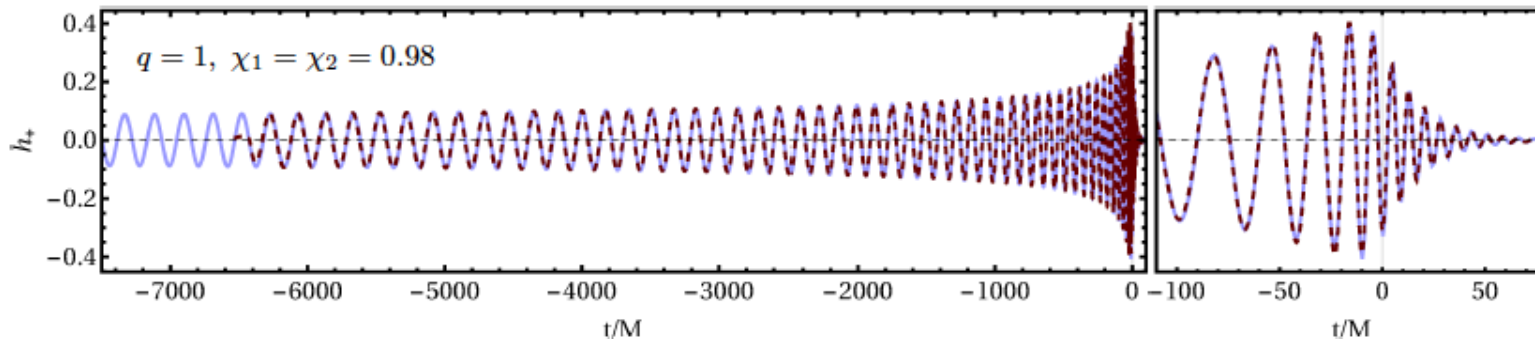
$$\phi_{\text{Int}} = \frac{1}{\eta} \left( \beta_0 + \beta_1 f + \beta_2 \text{Log}(f) - \frac{\beta_3}{3} f^{-3} \right).$$

$$\phi_{\text{MR}} = \frac{1}{\eta} \left\{ \alpha_0 + \alpha_1 f - \alpha_2 f^{-1} + \frac{4}{3} \alpha_3 f^{3/4} + \alpha_4 \tan^{-1} \left( \frac{f - \alpha_5 f_{\text{RD}}}{f_{\text{damp}}} \right) \right\}.$$

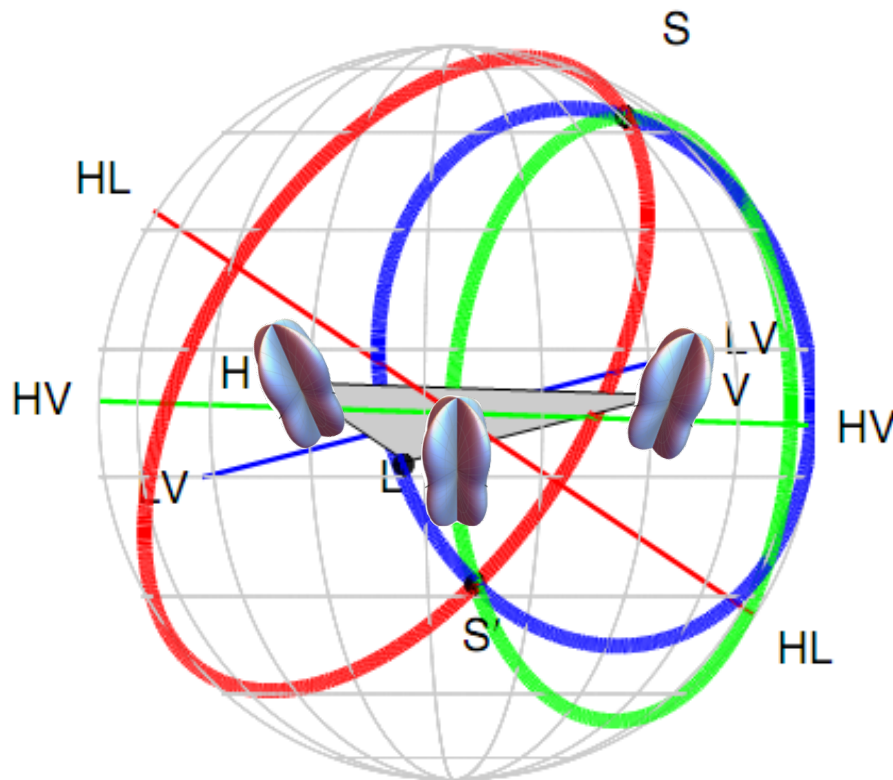
# Tests of consistency with predictions from General Relativity



- Matches between parametric models and NR waveforms can be better than 1%
- In the region of the parameter space appropriate for GW150914, tests based on parametric models are valid tests of GR



Measuring the response in *three non-co-oriented detectors* permits a measurement of GW polarization for the first time!



From the pattern of signal amplitudes in three detectors:

For GW170814  
(no optical counterpart),

Bayes factor (T/V) = 200  
Bayes factor (T/S) = 1000

Pure tensor is strongly favored over pure vector or pure scalar.

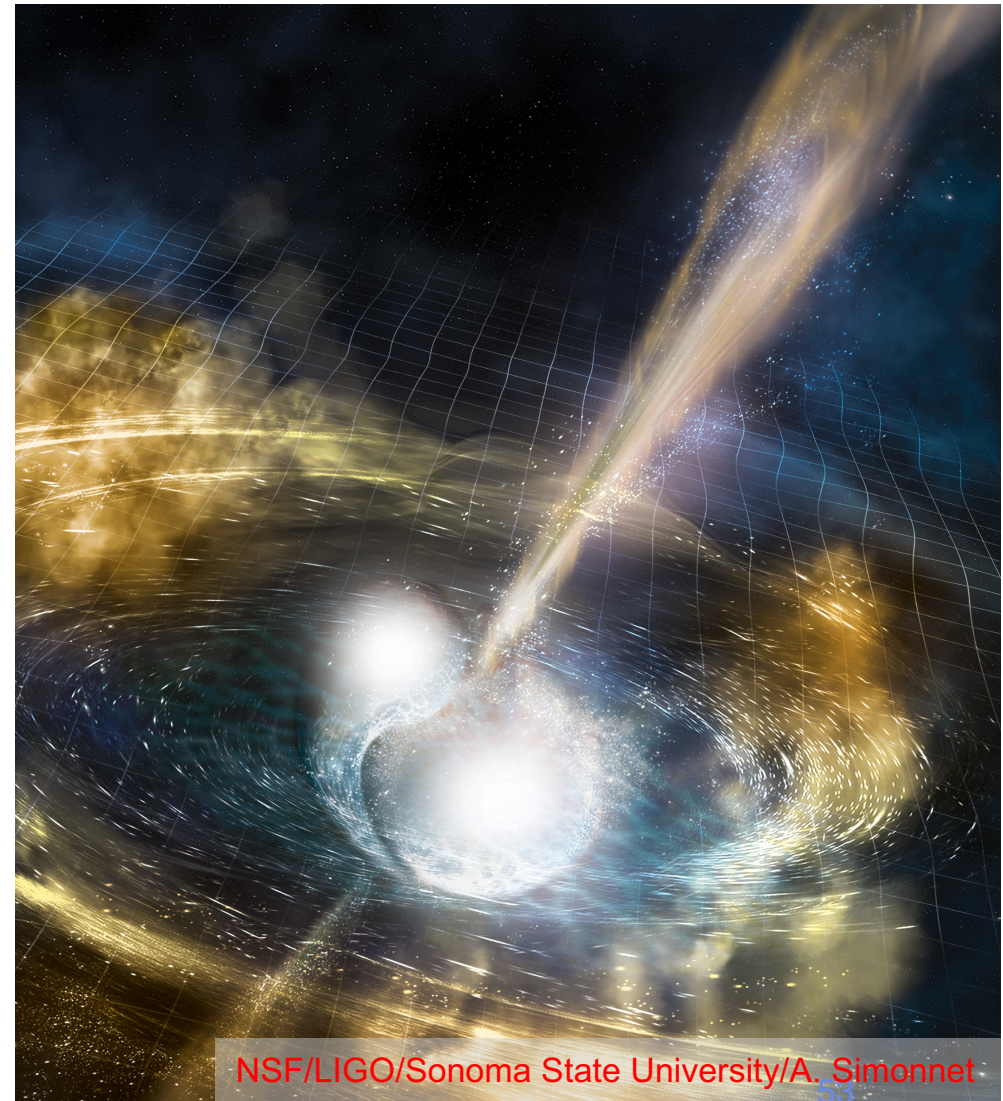
To measure small admixtures of S,V in dominant T requires *five non-co-oriented detectors*



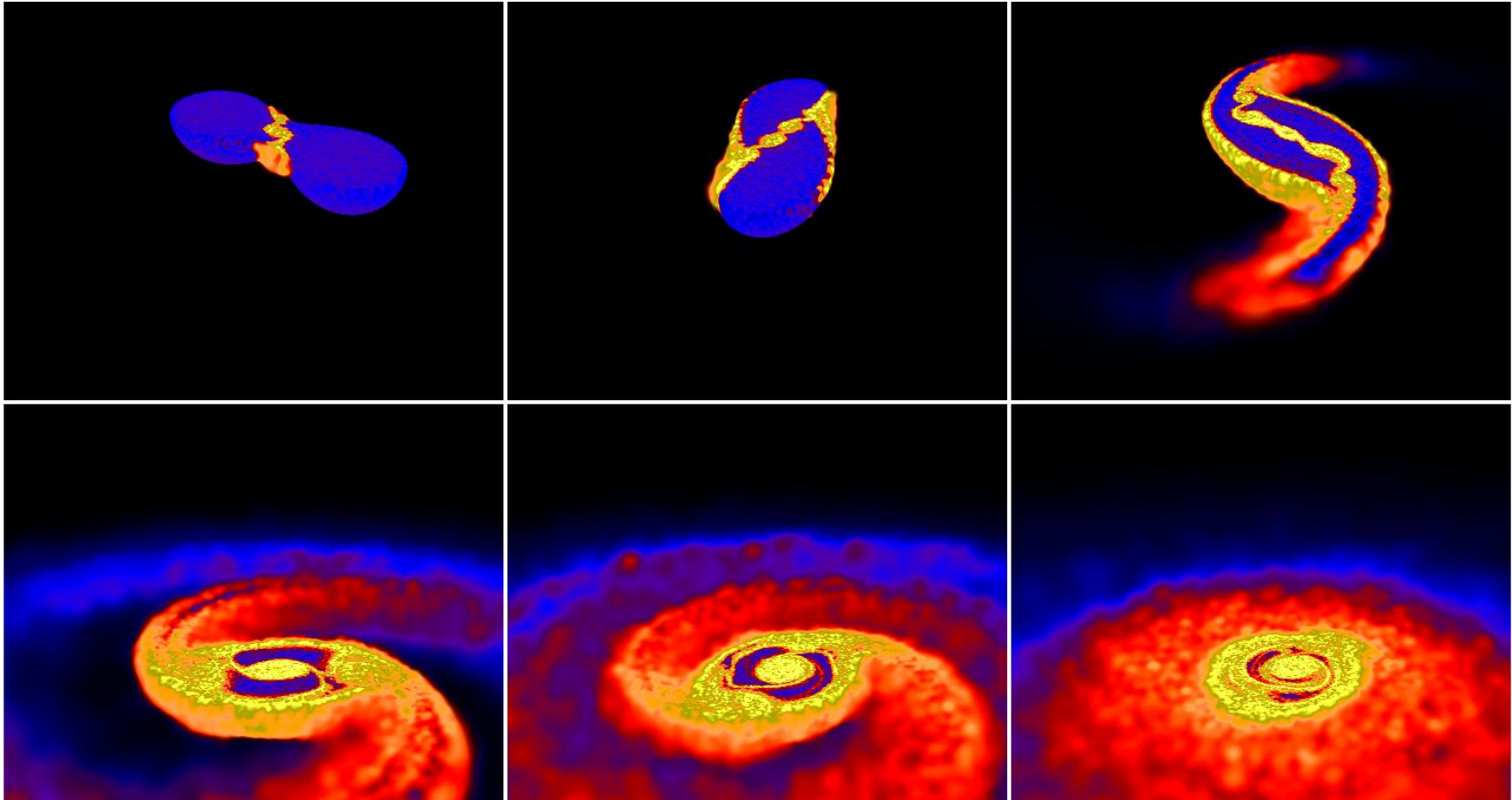
As the stars spiral together, they get torn apart by each other's gravity:  
Tidal distortion → Disruption!



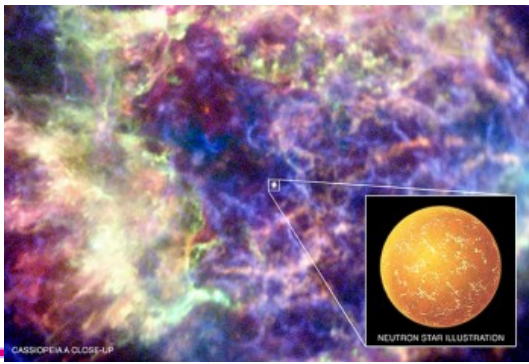
The disruption of the stars results in a huge outflow of neutron-rich “dynamical ejecta” that powers a GRB and broad-band afterglow



# BNS mergers, tidal distortion and disruption

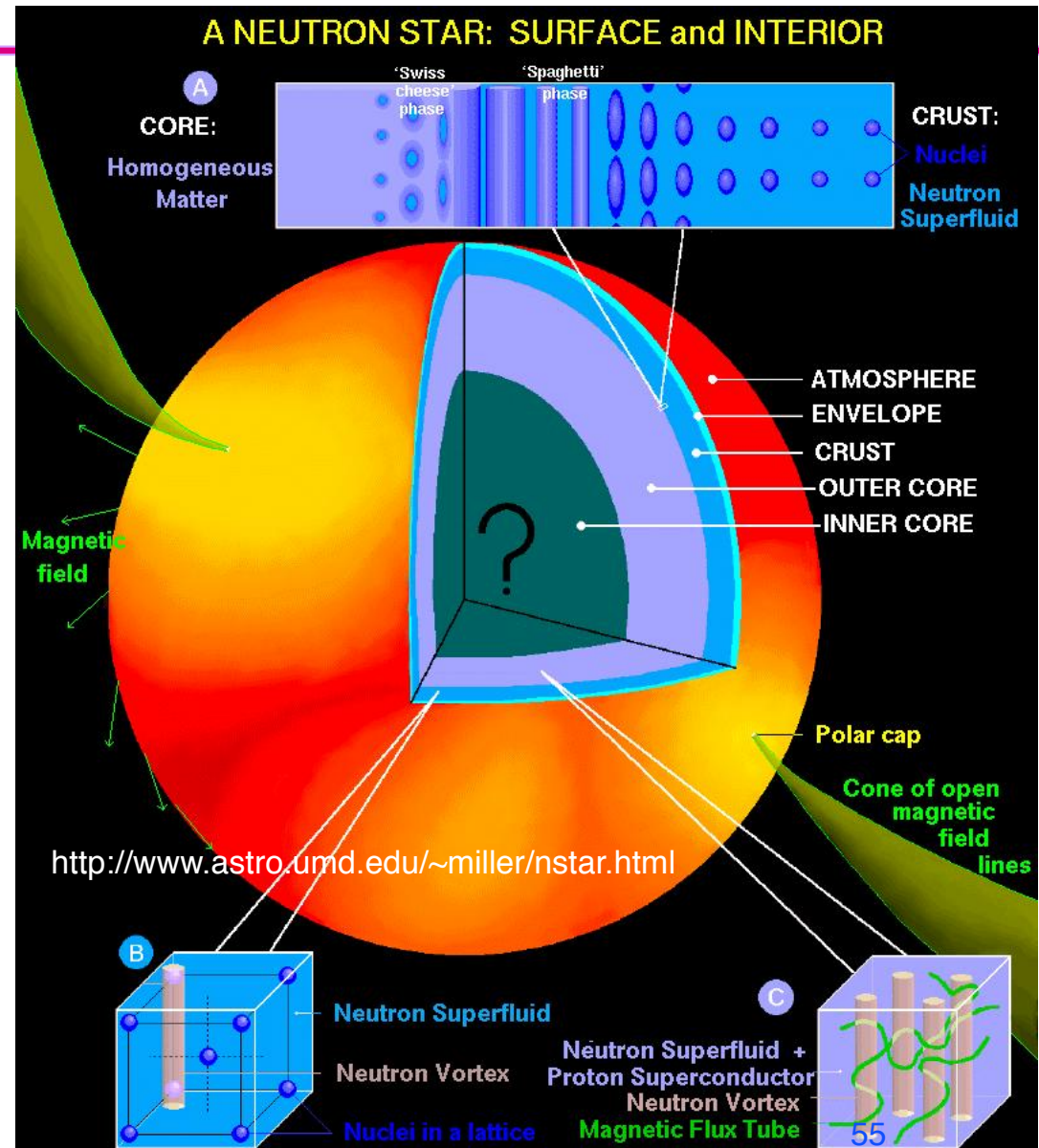
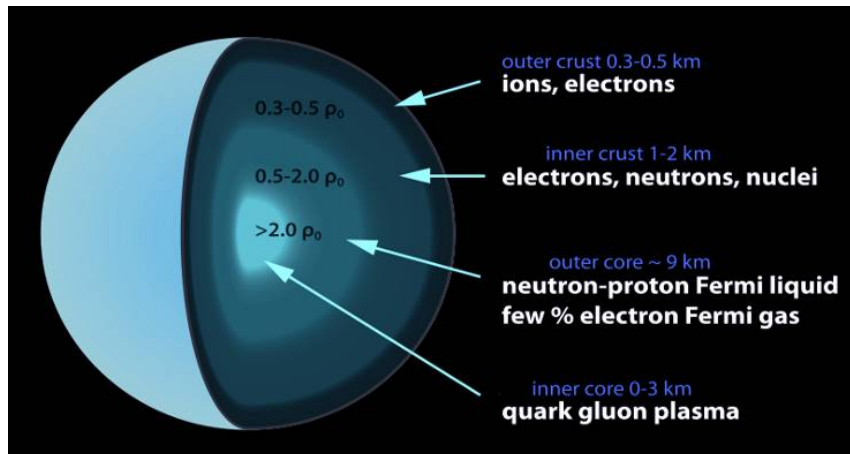


Credit: Daniel Price and Stephan Rosswog

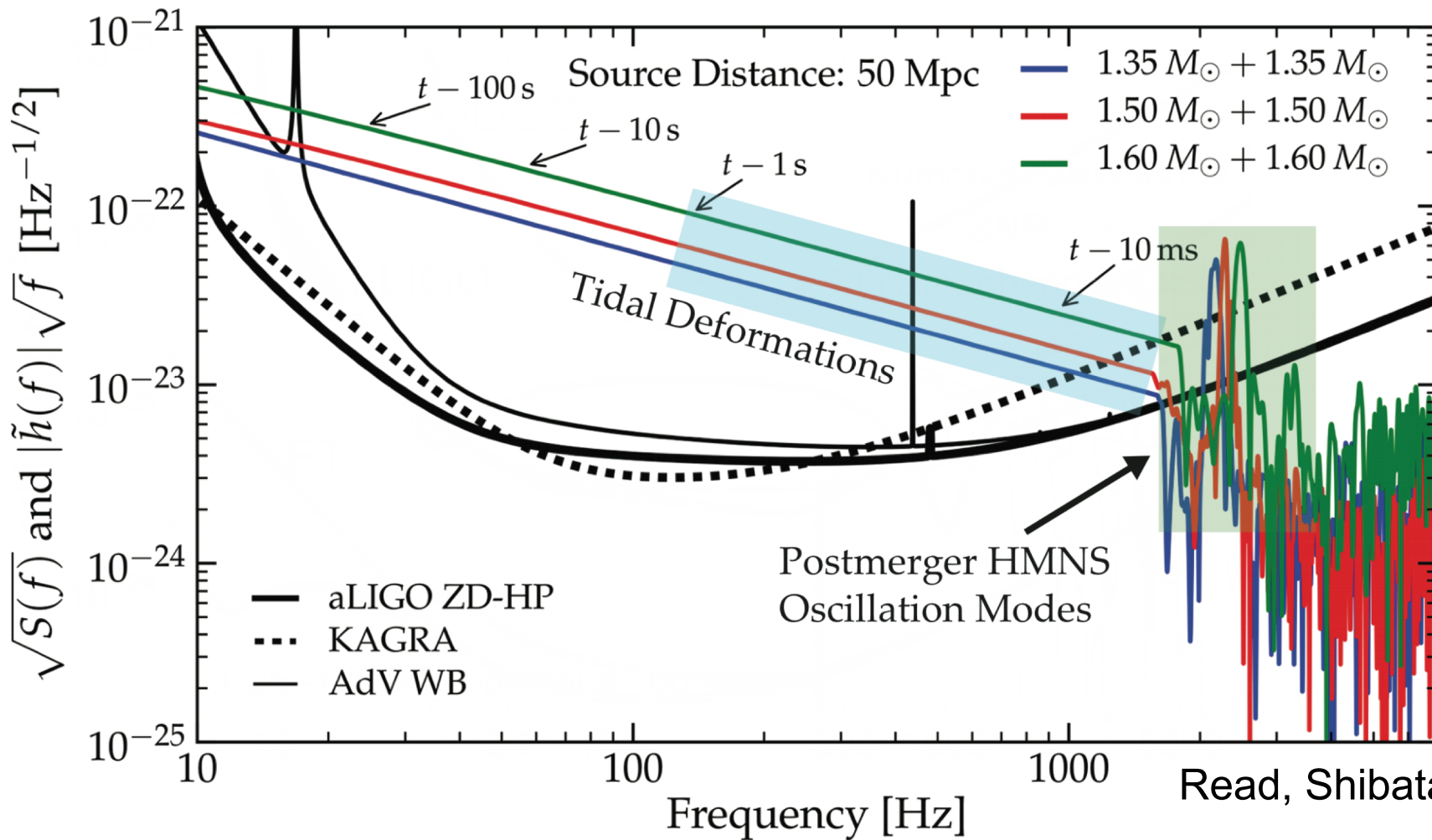


# Neutron stars

- Dead remnants of massive star core collapse supernovae
- A unique laboratory for fundamental physics
- All four forces of nature, Strong, Weak, EM, gravity – all under *the most extreme beyond-laboratory conditions*
- Structure can be revealed through binary mergers



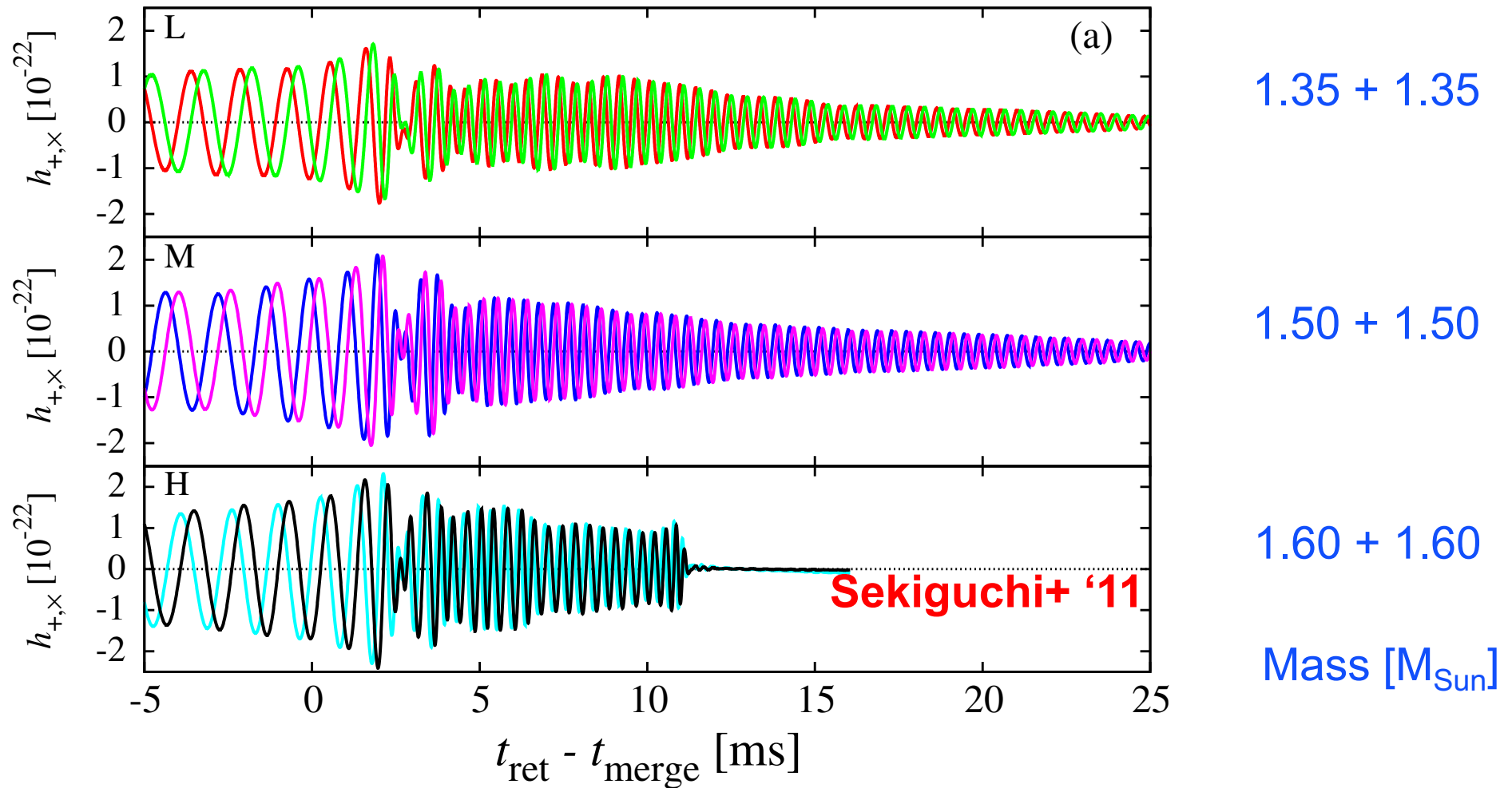
# Tidal disruption of neutron stars near merger



Read, Shibata, et al



# Nuclear Astrophysics: BNS Merger waveforms



Sekiguchi+ 11: First full GR NS-NS simulation with realistic microphysics, finite-temperature nuclear EOS of H. Shen+ '98, '11

# Formation mechanisms

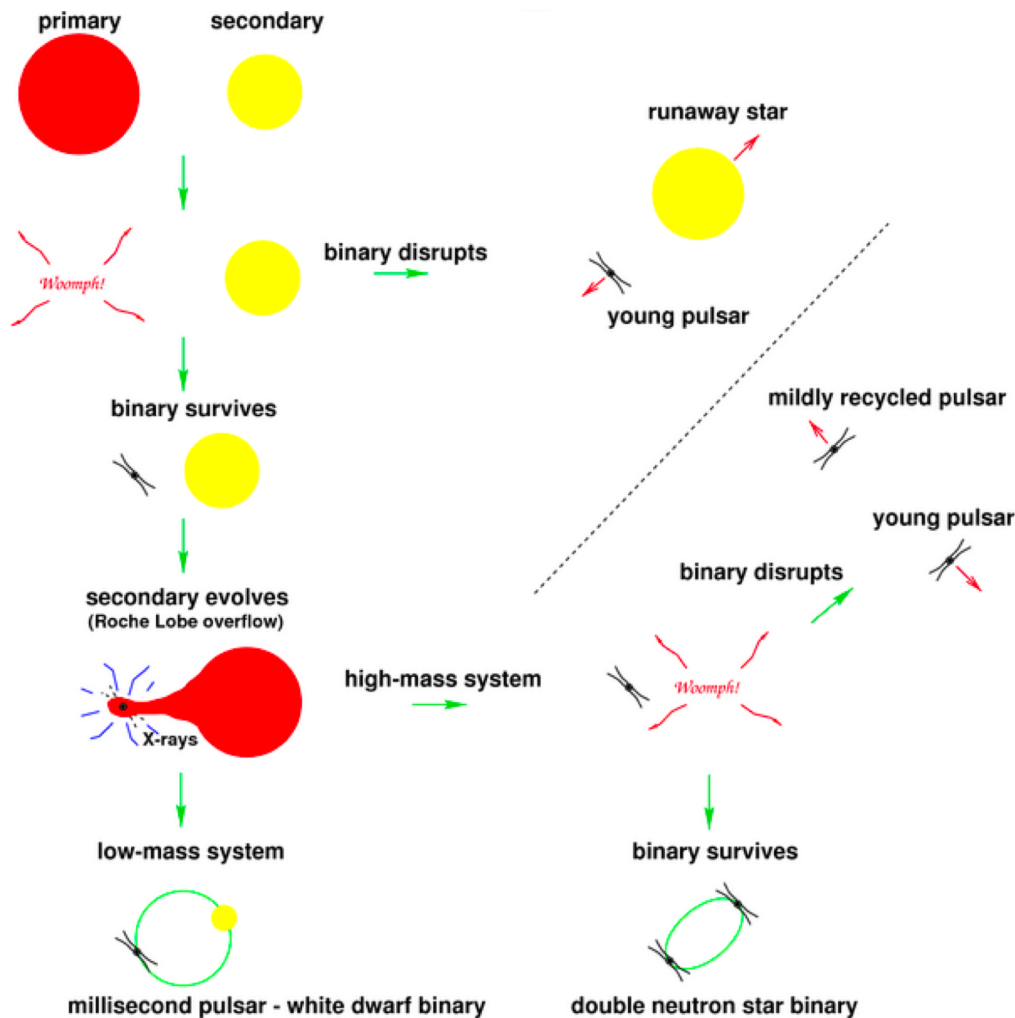
- How do massive binary black hole systems form?
- Common envelope evolution of isolated binaries: two massive stars survive successive CCSNe
- Dynamical capture of isolated black holes in N-body exchange interactions.
- Even the most massive stars ( $60-100 M_{\odot}$ ) can only produce black holes with mass  $> 20 M_{\odot}$  only in low-metallicity environments ( $\sim 0.1 Z_{\odot}$ ).

- <https://dcc.ligo.org/LIGO-P1500262/public/main>



# Formation channels

## Isolated binary



## Dynamical formation

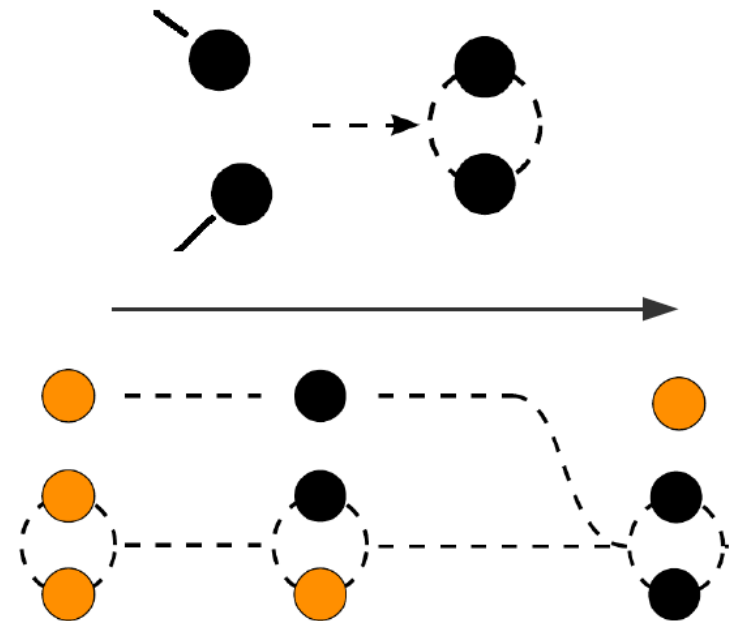
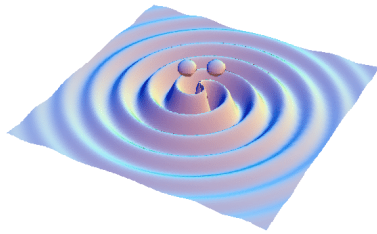


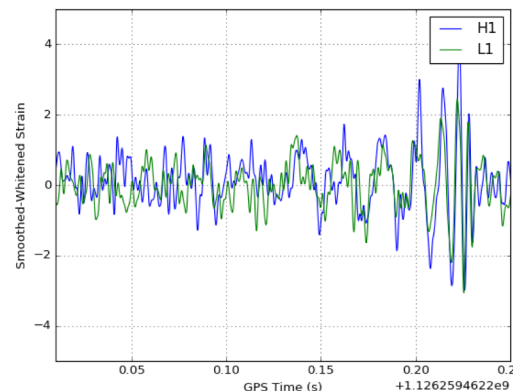
Fig. after Ziosi

Globular/young clusters/gal. nuclei



# Fun with CBCs!

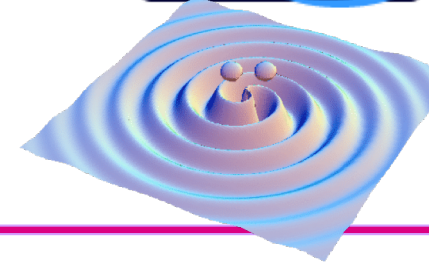
- GWs from compact binary coalescence is our most powerful probe of strong-field, highly-dynamical gravity.
- Fundamental physics:
  - » properties of GWs: energy loss during inspiral, spin-orbit dynamics, propagation speed, polarizations, dispersion, ...
  - » Powerful tests of GR as the fundamental theory of gravity
  - » Properties of nuclear matter under extreme conditions (NEOS)
- Astrophysics:
  - » merger rates, populations, masses of binary black holes
  - » merger rates, populations, masses and radii of neutron stars
  - » Formation mechanisms
  - » Production of heavy elements
  - » ...
- The fun is just beginning! **Join in!**





THANK YOU for your attention!

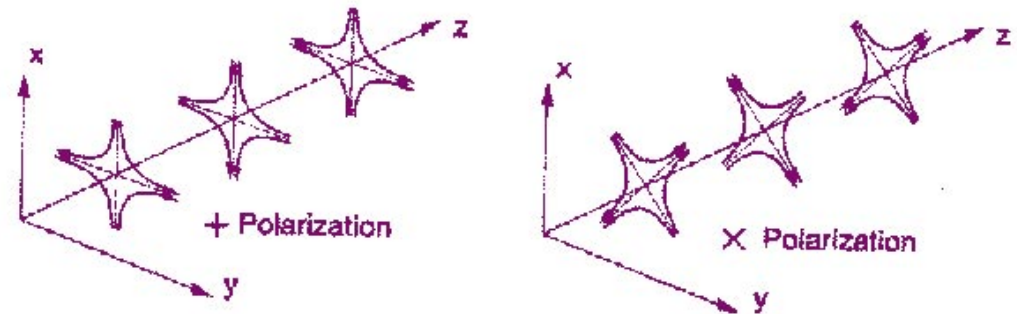
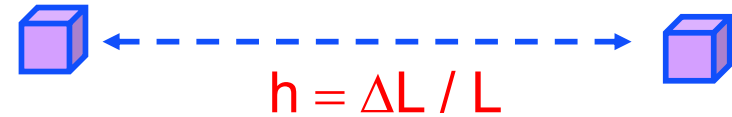
---



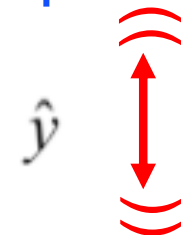
# Nature of Gravitational Radiation

General Relativity predicts that rapidly changing gravitational fields produce ripples of curvature in fabric of spacetime

- Stretches and squeezes space between “test masses” – strain  $h = \Delta L / L$
- propagating at speed of light
  - mass of graviton = 0
- space-time distortions are transverse to direction of propagation
- GW are tensor fields (EM: vector fields)
  - two polarizations: plus ( $\oplus$ ) and cross ( $\otimes$ )
  - (EM: two polarizations,  $x$  and  $y$ )
  - Spin of graviton = 2



Contrast with EM dipole radiation:



# Gravitational Waves

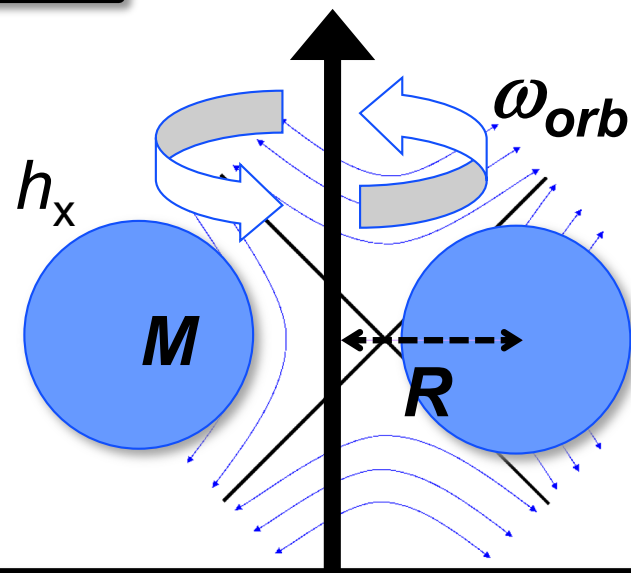
Solution for an outward propagating wave in z-direction:

$$h(t, z) = h_{\mu\nu} e^{i(\omega t - kz)} = h_+(t - z/c) + h_x(t - z/c)$$

$$h_{\mu\nu} \approx \begin{pmatrix} 0 & 0 & 0 & 0 \\ 0 & h_+ & h_x & 0 \\ 0 & h_x & -h_+ & 0 \\ 0 & 0 & 0 & 0 \end{pmatrix} \approx \frac{1}{r} \frac{G}{c^4} \ddot{Y}_{\mu\nu}$$

**Physically,  $h$  is a strain:  $\Delta L/L$**

$$h \approx \frac{8GM R^2 \omega_{orb}^2}{rc^4} \sim 10^{-21}$$

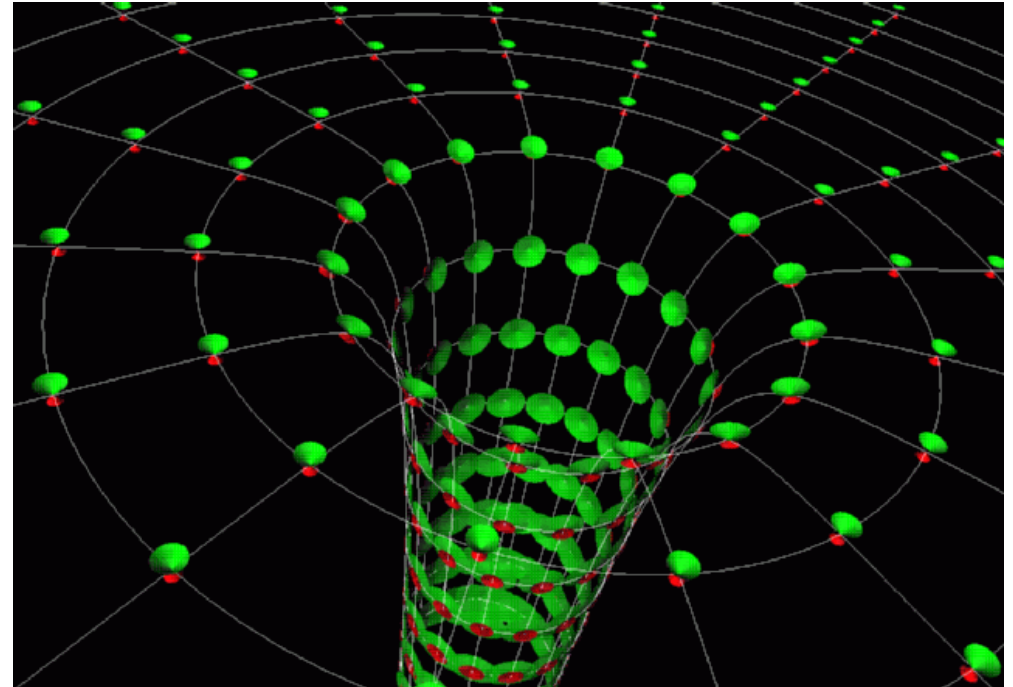


**Kepler 3<sup>rd</sup>:  $R^3 \omega_{orb}^2 = G M_{tot}$**

# Strong-field



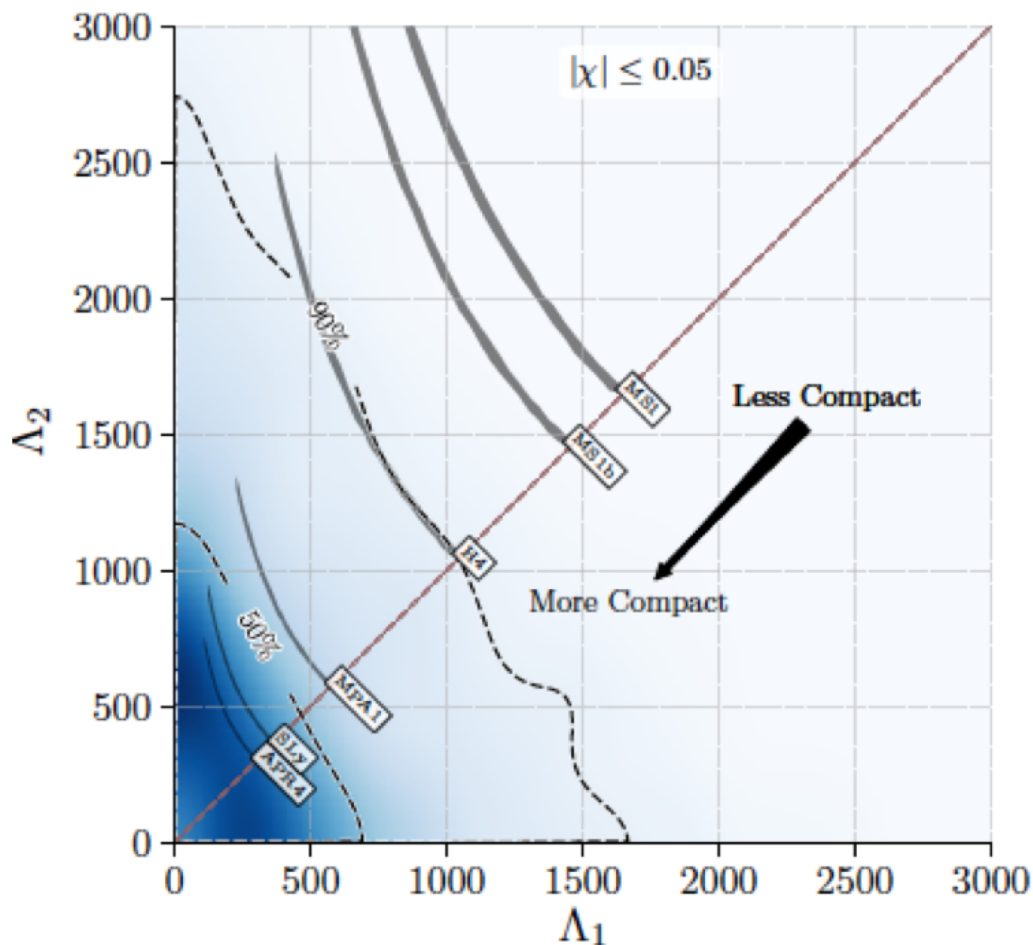
- Most tests of GR focus on small deviations from Newtonian dynamics (post-Newtonian weak-field approximation)
- Space-time curvature is a *tiny* effect everywhere except:
  - The universe in the early moments of the big bang
  - Near/in the horizon of black holes
- This is where GR gets *non-linear* and interesting!
- We aren't very close to any black holes (fortunately!), and can't see them with light or other EM radiation...



**But we can search for (*weak-field*) gravitational waves as a signal of their presence and dynamics**



# Constraints on tidal distortion



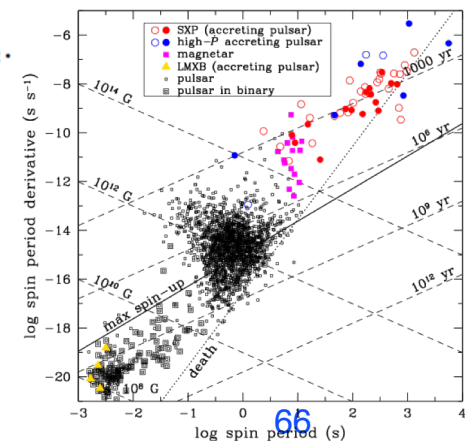
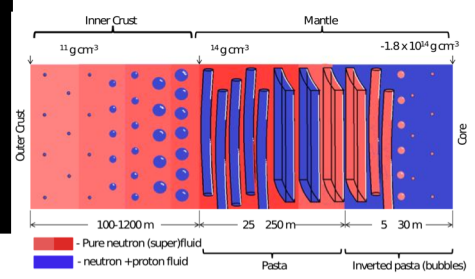
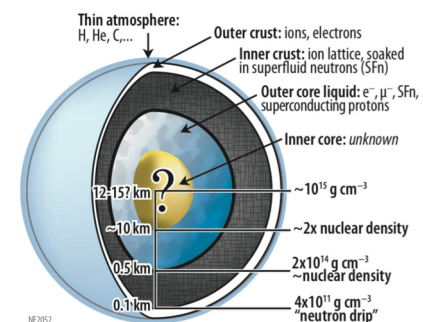
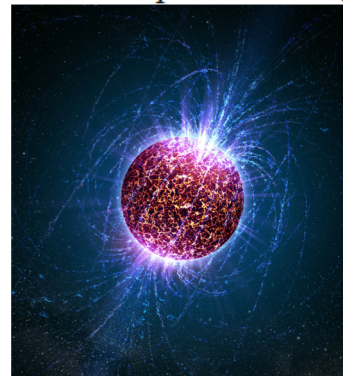
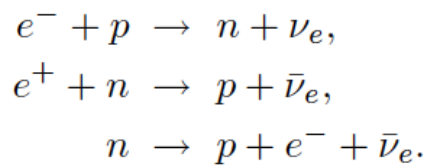
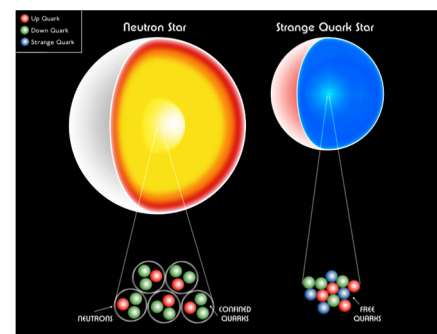
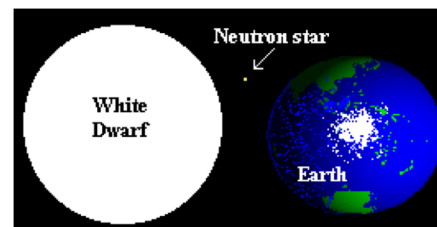
- Tidal deformability:

$$\Lambda = \frac{2}{3} k_2 \frac{c^2}{G} \left( \frac{R}{M} \right)^5$$

- $k_2$  is the 2<sup>nd</sup> Love number
- R and M are the radius and mass of the star
- LIGO results for GW170817 are most consistent with more compact stars,  $R < 14$  km

# All four fundamental forces under the most extreme conditions

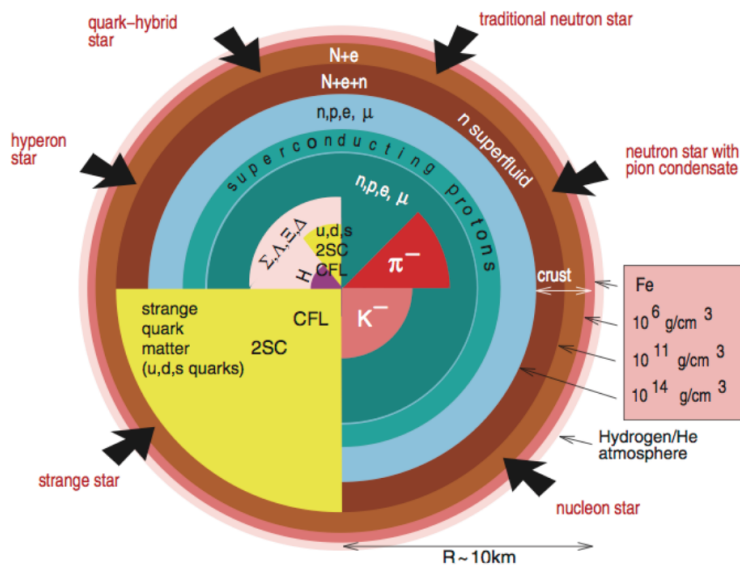
- **Gravity:** Compact stars have gravitational fields  $GM/c^2R \sim O(1)$ , strong tidal effects, strong curvature, highly relativistic
- **Strong interaction at  $> 2x$  nuclear density in core**
  - » Hard repulsive core of nucleon-nucleon interaction plays crucial role
  - » Potential transition to hyperonic matter, strange quark matter, QGP
  - » Complex ionic crystal lattice structure in crust: “nuclear pasta”
- **Weak interaction under extreme conditions with neutrino trapping -> beta equilibrium**
- **EM:** Superfluid core supporting extreme magnetic fields (perhaps  $> 10^{15}$  Gauss at surface), flux tube pinning in core



# NEOS, NS structure, and NS mass-radius relation

## Neutron Star Equation of State

- Simplification:  $T=0$ , pure neutron & proton gas. Appropriate (?) for interior of cold neutron stars.



C. D. Ott @ LVC Supernova Call, 2014/08/11

